IJCRT.ORG ISSN : 2320-2882

INTERNATIONAL JOURNAL OF CREATIVE RESEARCH THOUGHTS (IJCRT)

An International Open Access, Peer-reviewed, Refereed Journal

# SYNTHESIS SILVER NANAPARTICALS USING AQUEOUS EXTRACT OF TAMARINDUS INDICA FRUIT SHELL BY GREEN SYNTHESIS APPROACH

**[1]Shital Shivaji Kolhe, [2]Priti Devidas Lohakare, [3]Tushar Deepak Gaikwad, [4]Dr.Megha Salve**

[1]Student, [2] Student, [3] Student [4]Proffesor

[1]Pharmacy,

[1]Shivajirao Pawar College of pharmacy, Pachegaon,Maharashtra

**ABSTRACT**

The present study was carried out to synthesize silver nanoparticles (AgNPs) using the aqueous extract of *Tamarindus indica* fruit shell through an eco-friendly green synthesis approach. The fruit shell extract was subjected to preliminary phytochemical screening and GC-MS analysis to identify the bioactive constituents responsible for nanoparticle synthesis. Silver nanoparticles were synthesized using silver nitrate solution and characterized by various analytical techniques including UV-Visible Spectroscopy, FTIR, XRD, SEM, EDAX, TEM, SAED, and DLS analysis. The formation of silver nanoparticles was confirmed by the characteristic color change from pale yellow to brown and by the appearance of a surface plasmon resonance peak in the UV-visible spectrum. Phytochemical analysis confirmed the presence of alkaloids, flavonoids, tannins, phenols, saponins, terpenoids, glycosides, quinones, and carbohydrates. GC-MS analysis revealed several bioactive compounds with medicinal significance. Characterization studies demonstrated that the synthesized nanoparticles were predominantly spherical, crystalline, and well dispersed with nanoscale dimensions. The synthesized silver nanoparticles exhibited significant antioxidant activity as determined by DPPH radical scavenging assay, hydrogen peroxide scavenging assay, and total antioxidant capacity assay. Furthermore, the nanoparticles showed excellent antibacterial activity against both Gram-positive and Gram-negative bacterial strains, including *Staphylococcus aureus*, *Bacillus subtilis*, *Escherichia coli*, and *Klebsiella pneumoniae*. The study confirms that *Tamarindus indica* fruit shell, an agricultural waste material, can serve as an effective reducing and stabilizing agent for the green synthesis of silver nanoparticles with promising biomedical and environmental applications.

**Keywords:** Green Synthesis, Silver Nanoparticles, *Tamarindus indica* Fruit Shell, Phytochemical Screening, GC-MS Analysis, Characterization, Antioxidant Activity, Antibacterial Activity, Nanotechnology, Biomedical Applications.

## 1. INTRODUCTION

### 1.1 Introduction to Nanoscience and Nanotechnology

Nanoscience is an emerging multidisciplinary research area in the recent times. In the past few decades, the term 'nano' makes magic to the world by gaining attention, interest and inspired to scientists. Nanoscience is a multidisciplinary field; it includes physics, chemistry, electronics, mechanics, toxicology, surface science, computer science and molecular biology. Nanotechnology produces functionalized materials, tools and structures through a regulated process at a nanometer length scale. This involves the synthesis, characterization, discovery and use of nanostructured materials. It is a very important material for scientific reasons and practical applications. Nanoparticles are the basic components of nanotechnology. It is derived from the Greek word 'nano' meaning 'dwarf'. The scale is measured as on billionth of a meter or $10^{-9}$ m.

## 1.2 History of 'Nano'

People made fabrics with a network of pore sizes ranging from 1 to 20 nm thousands of years ago. The natural colors of henna and black hair were used by ancient Egyptians. Pasting acid, lead oxide and a small amount of water makes the hair dye look black. The British museum boasts the Lycurgus cup dragged the underworld by Ambrosia. It is one of the most fascinated pieces of Roman glasswork. It appears green while illuminated from outside (Figure 1.1 a). The cup appears ruby red during illuminated from inside and the King Lycurgus looks purple (Figure 1.1 b and c). The cup was analyzed by SEM and the result shows the presence of nanosized particles of silver with the percentage of 66.2 %, gold with 31.2 % and copper with

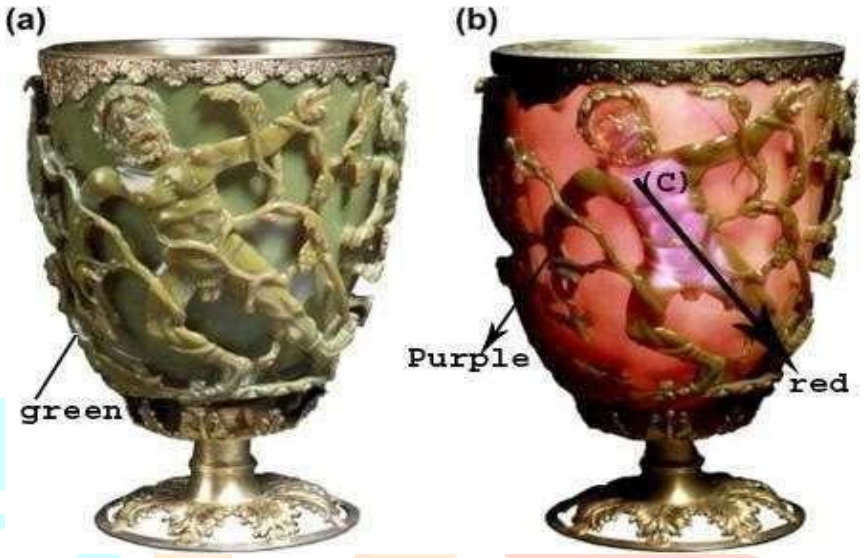


2.6 %. These three nanoparticles were combined together with the size up to 100 nm. These are embedded in the glass. The reflection of different colour of nanoparticles was due to absorption and scattering of light.

## 1.3 Nanoparticles

Nanoparticles were described as a small material with a size ranges between 1 and 100 nm and these nanoparticles act as a whole system with respect to its transport and properties. Nanoparticles are widely used in scientific studies and research in the 1970s and 1980s. Nanoparticles have size related properties and it differs significantly than bulk materials. Nanoparticles have variety of diversity such as metal, metal oxides, carbon materials, metal sulfides, semiconductor etc. Nanoparticles exhibit different morphological diversity such as rod, sphere, cylinders, cubes, hollow spheres, tubes, disks etc. Nanoparticles are the main components of nanotechnology for a variety of applications.

Nanoparticle exhibits various forms such as nanoclusters and nanopowders. Nanoclusters are characterized as materials with a range of between 1 and 10 nm with a narrow size distribution. Nanoclusters are a one-dimensional material. Nanopowders are defined as the collective type of ultrafine particles such as nanoclusters and nanoparticles (Fahlman 2007). Among the diversity of nanostructure, noble metal nanostructures receive a great deal of attention due to their unique properties, including significant optical enhancements and photothermal properties. The optical field improvement of nanoparticles is due to the high dispersion and absorption of light. This enhancement result shows that metal nanoparticles grow from the resonant oscillation of their collective free electrons in the presence of light known as Localized Surface Plasmon Resonance (LSPR) (Jain *et al.*, 2008). Noble metal nanoparticles were exhibit wide range of behavior at the atomic to bulk transition (Kreibig and Volmer, 1995).

## 1.4 Types of Nanomaterials

Nanomaterials are extremely small in size. Nanomaterials should be at least one dimension (100 nm or less). It can be of four dimensionalities such as

- 0 D (Zero Dimension)
- 1 D (One Dimension)
- 2 D (Two Dimensions)
- 3 D (Three Dimensions)

This occurs in single, merged, aggregated and agglomerated forms with circular, tubular and irregular shapes. Nanomaterials have a lot of applications in the area of nanotechnology. It has various physical and chemical properties using specific chemicals.

The nanaomaterials are distinguished by an ultra-fine grain size (< 50 nm) Nanomaterials may be generated with a variety of dimensionalities (Table 1.1) as defined by Richard W. Siegel (Figure 1.4).

**Table 1.1: Different Dimensionalities of Nanomaterials**

| Dimensions | Structures |
|---|---|
| 0 D | Spheres and Clusters |
| 1D | Nanorods and Wires |
| 2D | Nanofilms and Plates |
| 3D | Nanoparticles |

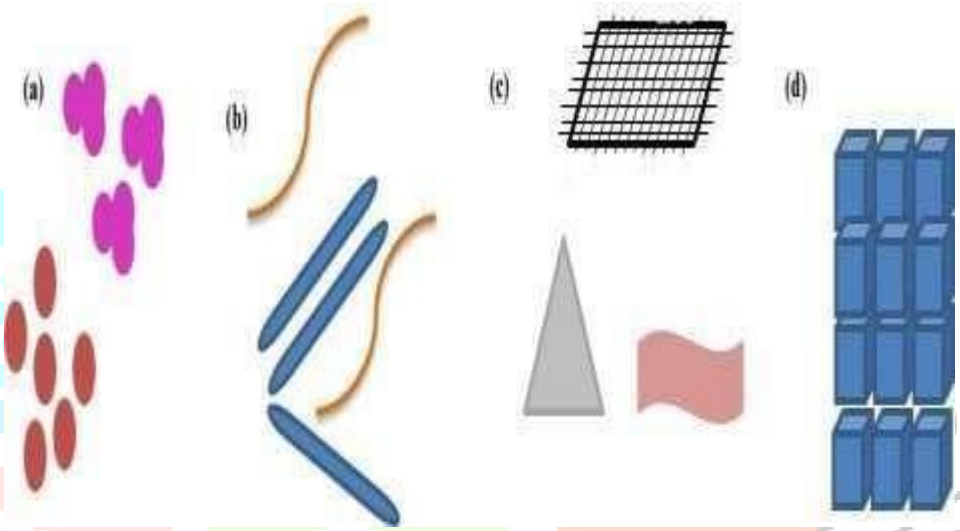


**Figure 1.4: Types of Nanomaterials**

**(a) 0 D (b) 1 D (c) 2 D (d) 3 D Nanomaterials**

## 1.5 Silver

Silver is a precious metal and is one of the best metals. Silver has attracted researchers because of its different properties. Silver is a white, soft, lustrous and transition metal. „Ag" is the chemical symbol of silver and it is the derivative of
„Argentum". The atomic number of „Ag" is 47 and atomic mass is 107.87. This metal is positioned at 47 in the periodic table. It is found in the crust of the earth in its pure and free elemental form. It is present in the form of alloy with other metals. Pure silver is ductile, malleable. It has strong conductivity property such as electrical and thermal conductivity and also reflectivity of other metals. And also it has lowest contact resistance (Nordberg *et al.,* 1998). Silver has used in medicinal system reported since 100 B.C. Silver has been highly utilized for thousand years ago in human history. It is widely used in jewels, utensils, currency, dental alloy and photography and explosives applications. In traditional Chinese and Indian Ayurveda medicinal system, Silver is considered as health additive (Singh *et al.,* 2008). Silver and its derivatives were used as disinfectants and microcides. It is used in wound dressing and preparing bandages.

## 1.6 Nanosilver

Nanosilver is a promising nanotechnology product. Preparing silver nanomaterials is a key feature of modern nanotechnology research. A great deal of attention has been paid to the physical, chemical and biological properties of silver nanoparticles due to their catalytic activity and bactericidal effects (Fayaz *et al.,* 2010; Sharma *et al.,* 2009). It is used as antimicrobial agents in wound dressings (Singh and Singh, 2014; Habiboallah *et al.,* 2014; Nambiar and Bhathena, 2010), topical creams used to prevent wound infections (Tian *et al.,* 2007) and anticancer agents (Kaur and Tikoo, 2013). The metallic silver has well known biological activities whereas the nanoscale silver may be even more effective.

## 1.7 Properties of Silver Nanoparticles

The electrical, thermal and optical properties of silver nanoparticles are different. It is used by incorporating with various products. Silver based compounds are nontoxic, inorganic and antimicrobial agents. Physical, chemical and biological properties of nanostructured silver were significant when compared to their macroscaled materials. The high use of silver nanoparticles is due to low sintering temperatures, high electrical conductivity and stability.

### 1.7.1 Optical Properties

In the fields of sensors and other devices, the optical properties of silver nanop articles have attracted great attention. Silver nanoparticles are capable of absorbing and dispersing light. The absorption and dispersion of light depends on the nanoparticles ' size and shape. Due to their electron conductivity on the metal surface, the intense interaction between silver nanoparticles and light occurs. It undergoes mutual oscillation at specific wavelengths during an excited state of light. This oscillation is called Surface Plasmon Resonance Effect (SPR) (Figure 1.5). The change of the maximum SPR from shorter wavelength to longer wavelength is a special feature of spherical particles. This is due to an increase in refractive index and particle size near the surface of the material.

### 1.7.2 Biological Properties

Surprisingly, there are strong biological activities of silver nanoparticles. In many textiles, bandages, wound dressing, and biomedical products, these are primarily used in antimicrobial coatings. Silver nanoparticles have been used to track the growth of different microorganism groups that cause several diseases. Some microorganisms were attained resistant to antibiotics due to frequent usage. Silver nanoparticles introduced into microbial cells can induce the high level of structural and morphological changes leads to cell death. In drug delivery systems, silver nanoparticles have the efficiency to release silver ions which kill the microbes. Silver nanoparticles exhibit wound healing, anticancer, antibacterial, antiviral, anti-inflammatory and antioxidant activity.

## 1.8 Methods Used for Preparation of Nanoparticles

The "bottom-up" and "top-down" approaches are basically two types of methods to be used for the preparation of nanoparticles (Figure 1.6).

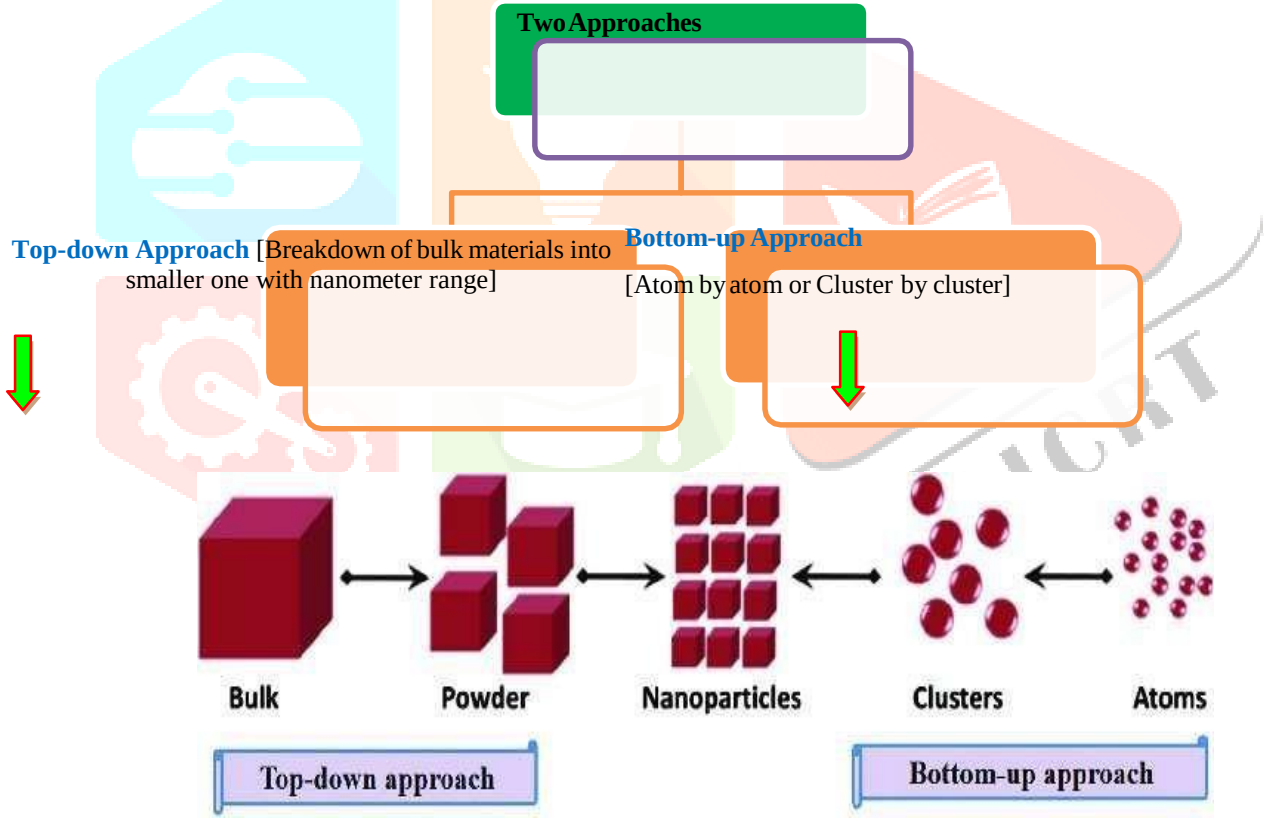


**Figure 1.6: Methods Used for Nanoparticles Synthesis**

The main drawback of this approach is it cannot prepare nanomaterials with controlled or desired properties. Top-down approach is defined as synthesis of nanomaterials starts with bulk materials and ends in the nanoscale materials formation via series of degradation process. The limitation of this approach is low reproducibility.

#### 1.8.1.1 Inert Gas Condensation

This technique is highly used to produce metallic nanoparticles. The vacuum chamber contains reduced inert gas. The metal is evaporated in this chamber, the metal reached super saturation through condensation process and gives nanosized particles. These particles are deposited on a substrate.

#### 1.8.1.2 Physical Vapour Deposition

In this process a metal vapour was deposited on electrically conductive materials as alloy coating. Thin films are produced by the conversion of condensed phase to vapour phase and undergo thermal treatment at inert atmosphere.

#### 1.8.1.3 Laser Pyrolysis

Laser pyrolysis was used to prepare ultrafine particles. Particles are prepared by heating a metal vapour and inert gas using laser. The metal vapour gets decomposed and initiates the nucleation of nanoparticles.

#### 1.8.1.4 Flame Spray Pyrolysis

This method used to produce highly purified metal oxide nanopowders. The precursor metal solution is sprayed through capillary tube and flow into a flame. The solvent burns inside the flame and then small droplets are formed. Metal oxide atoms were aggregated into nanoparticles which are collected on the substrate. The main advantage of this technique is synthesis of very fine particles (Gagan J and Pelagia-Irene G 2017).

#### 1.8.1.5 Melt Mixing

A molten stream of metal was subsequently mixed at high velocity with turbulence form of nanoparticles. It keeps the nanomaterials inside the glass. Metals cool down and form into nanoparticles. Mostly nanocomposite materials are synthesized through this technique.

#### 1.8.1.6 Ball Milling

It is the simplest method of nanoparticles synthesis. Planetary, vibratory and tumbler types of mills are used. The container filled with carbide balls in the ratio of 2:1. The container is rotated around horizontal axis at high speed under vacuum condition and it produces nanosized materials. This method is used to produce metallic and ceramic nanoparticles (Thakur Prasad Yadav *et al.,* 2012).

#### 1.8.1.7 High Energy Ball Milling

The precursor material is placed in a high energy mill along with a suitable medium. The precursor was reduced in their size and produce colloidal nanoparticles. The main disadvantage of this technique is contamination of the material is possible (Numan Salah *et al.,* 2011).

### 1.8.2 Chemicals Techniques

#### 1.8.2.1 Sol-gel Approach

Sol-gel approach is nothing more than the process of preparing liquid phase (sol) colloidal nanoparticles (gel). It is an approach to wet chemical synthesis and is used for oxide and composite nanomaterial preparation. This process has taken four phases such as hydrolysis, gelation, precipitation and hydrothermal (Kung HH and Ko EI 1996). The main advantage of this approach is storage at low temperatures, durability, consistency and cost-effectiveness. Disadvantage is the risk of synthetic chemicals contamination.

#### 1.8.2.2 Hydrothermal Synthesis

In this process, synthesis takes place at the boiling point of water in aqueous solution. This process is carried out in closed containers or high-pressure autoclaves. Due to low cost and energy consumption, these processes can be scaled up for industrial use. $TiO_2$ photo catalysts have been synthesized by hydrothermal processes among numerous examples (Ren *et al.,* 2007).

#### 1.8.2.3 Laser Ablation

It is used to synthesis of colloidal nanoparticles and magnetic nanoparticles using various solvents. The bulk metal plate has been dipped into a liquid medium and passes by laser and creates nanoparticles through a plasma plume condensation (Mafune *et al.,* 2001).
Disadvantage: - It required higher energy
- It needs growth rate control of magnetic nanoparticles.

#### 1.8.2.4 Solvothermal Synthesis

The reaction in the solvent-thermal process is conducted ta temeratures (200 - 300 °C) above theri boiling point in organic solvents. Solvothermal reactions are performed under subcritical or supercritical solvent conditions in a specially closed container or high pressure autoclave. Under these conditions, the reactive solubility increases significantly, allowing reactions to occur at lower temperatures. The solvent thermal process allows the choice of different solvents of their combination, thereby increasing the versatility of the synthesis. For example, in a blend of solvents Hydrogen Fluoride (HF) and 2-propanol well -defined $TiO_2$ nanocdrystals with high reactivity have been synthesized (Yang *et al.,* 2008).

#### 1.8.2.5 Reduction Method

The chemical reduction process is the most common technique of nanoparticle preparation. Reducing agents have been used such as sodium borohydride, trisodium citrate, hydrazine hydrate and ascorbic acids. The reduction agents converted silver ions ($Ag^+$) into silver nanoparticles ($Ag^0$). Sometimes agglomeration of particles was occurred. It gets reduced by the usage of protective agent. The protective agents are otherwise called as capping agents. These agents were bound on the surface of the nanoparticles and produces individual particles.

#### 1.8.2.6 Drawbacks of Physical and Chemical Methods

Both the methods are very cost effective. These methods require reducing agents as well as capping agents. Some of these agents are highly toxic to environment, flammable, need high energy, pressure, temperature and it cannot be easily disposable. So that, green synthesis method is commonly available, single step procedure and preferred to prepare nanoparticles. Green synthesis method was performed using microbes and plants and their products. This method is most adorable due to economically relative, nontoxic and environmental benign.

### 1.8.3 Biological Methods

Biological methods or green methods are used to transform metal to metal nanoparticles using natural capping, reducing and stabilizing agent. In this process, depending on various environmental factors such as pH, temperature, light, concentration of the substrate, etc., the shape and size of controlled synthesis is possible. Green synthesis method is achieved by employing plant and microorganisms. Some of the microorganisms are bacteria (Gurunathan *et al.,* 2009), fungi (Mukherjee *et al.,* 2002; Sastry *et al.,* 2005), actinomycetes (Saminathan 2015), algae (Rajeshkumar *et al.,* 2012; Govindaraju *et al.,* 2008) and yeast (Kowshik *et al.,* 2003). There are two forms of microbe-mediated synthesis: intracellular and extra cellular. However, this method shows slow rate of synthesis and difficult to prepare in large scale and also it require culture maintenance and special handling compared to plant based synthesis process. Plant parts such as leaf (Sangeetha *et al.,* 2011; Yilmaz *et al.,* 2011; Joseph and Mathew 2015; Cruz *et al.,* 2010), callus (Satyavani *et al.,*), stem (Sathiskumar *et al.,* 2009), roots (Behravan *et al.,* 2019), fruits (Kumar *et al.,* 2017; Moldovan *et al.,* 2016) and peel (Ibrahim 2015). Plant materials are easy to use, biocompatible, non-toxic and safe to use. In the green synthesis process, plant extract acts as both a reduction and a capping agent.

## 1.9 Applications of Silver Nanoparticles

Several functions, such as larvicidal, catalytic, antimicrobial, anticancer and wound healing, etc., have unique properties of Silver nanoparticles (Figure 1.8).radicals were otherwise referred to as reactive oxygen species (ROS) which cause damage to lipids, carbohydrates, enzymes and nucleic acids. The damages and oxidative stress leads to cell injury and it implicated into ageing. It causes degenerative diseases including heart disease, diabetes, liver damage, cancer and inflammation. Silver nanoparticles shown excellent antioxidant and considered as alternative chemotherapeutic agent.

### 1.9.2 Catalytic Property of Silver Nanoparticles

Currently, Nanomaterials are used in wastewater treatment as disinfectants which released from factories (Das *et al.,* 2013). Nanomaterials prevent colonization of bacteria and eliminate from food and textiles. Dyes are released from textile, leather, and paper industries during processing stage. They are toxic to environment, non-biodegradable and removal of dyes from wastewater is a challenging problem. The most commonly used methods of dye adsorption include activated carbon, electro-coagulation and microbial treatment. Such methods reveal inconsequential degradation effects on a variety of toxic colors. SNPs were used for catalytic degradation of dyes like methylene blue (Vanaja *et al.,* 2014) and eosin Y (Vidhu and Phillip 2014). Silver nanoparticles have reported increased dye degradation capacity because of high surface area to volume ratio properties.

### 1.9.3 Antimicrobial Property of Silver Nanoparticles

Applications of nanoparticles are depends on their properties like electronic, optical and size and shape controlled properties. Among the metallic nanoparticles SNPs are commonly used in the medical field. SNPs have attracted great attention as antimicrobial agents to multidrug resistant pathogenic bacteria, in particular *E.coli* and *S. aureus*. Nanoparticles have the efficacy to bind microorganisms to the cell was and suppress their metabolic activity. Iron and iron oxide nanoparticles were extensively used in cell labeling, drug delivery and discovery, MRI scan and tissue repair. Silver and gold nanoparticles exhibit anticancer efficacy with limited therapeutic applications (Huang *et al.,* 2015). Nanoparticles antibacterial activity depends on the size, shape and availability of the surface area. Ibrahim (2015) reported that antibacterial efficacy of peel extract mediated silver nanoparticles against four different pathogenic bacteria"s and dermatophytes like *Candida albicans*. Silver nanoparticles have also been used in the medical field to treat burnt wounds and other types of infections. Silver nanoparticles exhibit higher antibacterial activity compared to bulk metallic silver (Morones *et al.,* 2005).

### 1.9.4 Anticancer Property of Silver Nanoparticles

Cancer is an irregular development of cells that can invade and spread to different place of the body. Various cancers are categorized on the basis of origin. Main types of cancer are *carcinoma* formed on the surface of organs and glands, *sarcomas* develop in fat, muscles, joints, bones and nerves and *leukemias* is the development of cancer of the blood. Breast cancer mostly affects the women it notices a mass or tumor in the breast. Diagnosis of cancer was done by using MRI scanning. Mostly, breast cancer is affecting the women between 30-44 years. The risk of breast cancer was reduced by combined surgery with other treatment methodologies such as chemotherapy, radiation therapy, behavioral therapy and hormone therapy. Such treatment procedures often destroy normal cells at high cost. Nanoparticles play a vital role in oncology field. Silver nanoparticles were used to deliver cancer drugs into their targets (Ravindran *et al.,* 2013).

## 1.10 Plant Source

### 1.10.1 *Tamarindus indica* – Scientific Description

**Kingdom** : Plantae
**Class** : Liliopsida – Monocotyledons
**Order** : Fabales
**Family** : Fabaceae / Leguminosae
**Subfamily** : Caesalpinioideae
**Genus** : *Tamarindus*
**Species** : *T. indica L.*

### 1.10.2 Description

*Tamarindus indica* L. is the member of the Caesalpiniaceae subfamily of Fabaceae family and commonly known as tamarind fruit. It is an evergreen monotypic species. The native of this plant is Africa and now highly planted in India. This tree has grown even in dry regions of long duration. It is a slow growing tree and grows up to 25 meters high. Tamarind seeds are very hard, brown in colour and protected with an endocarp layer.

**Figure 1.11: Tamarind Tree, Fruit, Pulp and Shell**

Tamarind tree is a multipurpose tropical tree and it consumed mostly for its fruits. Fruits have been eaten as raw or processed for food purpose. The geographical distribution of this plant is subtropics and semiarid tropics. Tamarind


has been used as a medicinal plant for centuries; its fruits are the most valuable part and have often been recorded as curative in a variety of pharmacopoeias. The parts of the Tamarind plants are seeds, fruits and leaves; they are used in traditional medicines for the treatment of various diseases (Figure 1.11).

### 1.10.3 Phytochemical Constitution of Tamarind

Tamarind contains carbohydrates like glucose, fructose, galactose in pod. Fats, vitamins, organic acids, and fiber are rich in fruit. Leaves contain flavonoids, terpenes, aromatic compounds and alkaloids. Pulp of this plant fruit is used for many medicinal purposes and food. The taste of the fruit pulp is sour and slightly acidic in nature. The plant contains the glycosides: vitexin, isovitexin, orientin and isoorientin. The bark yields the alkaloids and hordenine.

### 1.10.4 Medicinal Uses

Tamarind was gives relief from constipation. Tamarind leaves were boiled and used as poultices for swollen joints and also applied to foreheads of fever fatalities. Tamarind fruit exhibits laxative and carminative effects because of the presence of malic acid, tartaric acid and potassium bitartrate. The fruit pulp is effective for digestion and remedy for bile disorders and rheumatism. Tamarind has polyphenols which is responsible for antioxidant and anti-inflammatory

activity. It can protect from heart disease, cancer and diabetics. The seed extract may help reduce the blood sugar and pulp extract involves in the reduction of loss of body weight and reverse fatty liver disease.

## 2. AIM, SCOPE AND OBJECTIVES

To synthesize silver nanoparticles using the aqueous extract of *Tamarindus indica* fruit shell by a green synthesis approach.

### 2.1 Definition of the Problem

Metal Nanoparticles have important applications in all fields. The design of low cost and over yield methods for the synthesis of nanoparticles is, therefore a significant task. Current methods for producing nanoparticles require tough and toxic chemicals. It is therefore essential to grow eco-friendly sustainable alternatives to current chemical methods. Plant-based synthesis of metal nanoparticles which substitute a few of the existing chemical methods as well as physical methods used to produce nanoparticles. Nonetheless, some problems need to be resolved before such biosynthetic procedures can compete with existing methods. Silver nanoparticles have achieved a special focus among several noble metal nanoparticles

1. Normally, Silver nanoparticles are synthesized using chemicals, these chemicals acts as reducing agents, which later become responsible for different biological hazards because of their common toxicity; creating severe concerns about the development of environmental friendly processes. Therefore, to solve the objective; biological approaches are emerging to fill the void. The present research discusses the vast diversity of plants to be used for the rapid and single-step protocol preparation process with green concepts over conventional ones and explains the specific biomedical and catalytic activities of Silver Nanoparticles.
2. Green Chemistry should aim to prevent waste, reduce energy use, use recycled materials and implement methods that minimize risk. The three key principles for the preparation of nanoparticles in a green synthesis method are the choice of solvent medium (preferably water), environmental-friendly reducing agent and non-toxic substrate for the stabilization of nanoparticles. The present research focuses on groundbreaking research into silver nanostructures synthesis using plant extract as a reducing and capping agent.
3. Tamarindus indica fruit shell accounts for more than 60 per cent of domestic waste. Tamarind fruit shells pose serious problems for the local environment in terms of disposal.
4. The novelty of this research is reutilization of the domestic waste material in the form of nanoparticles.

### 2.2 The scope of the Investigation

The present investigation reveals that, green synthesis of Silver Nanoparticles and the potential of the fruit shell of the pharmacologically essential tree Tamarindus indica.

1. To screen the bioactive substances (Phyto-chemicals) present in the aqueous extract of *Tamarindus indica* fruit shell by preliminary *phytochemical screening* methods and Gas Chromatography-Mass Spectrum (GC-MS).
2. To synthesize the Silver Nanoparticles by elaborating and standardizing the existing green methods of synthesis.
3. To characterize the synthesized Silver Nanoparticles by using different characterization techniques like UV-Visible, Fourier Transform Infrared Spectroscopy (FTIR), Energy Dispersive Analysis X-Ray (EDAX), X-ray Diffraction (XRD), Scanning Electron Microscope (SEM), Transmission Electron Microscope (TEM) and Dynamic Light scattering (DLS).
4. To investigate the antioxidant, antibacterial and anticancer activity of the synthesized Silver Nanoparticles.
5. To examine the catalytic activity of the synthesized Silver Nanoparticles by degrading hazardous dyes like Saffranin O and Methylene blue.

## 3. EXPERIMENTAL METHODOLOGY

### 3.1 Chemicals

Analytical grade Silver Nitrate, DPPH (2,2-Diphenyl-1-Picrylhydrazyl), Ammonium Molybdate, Hydrogen Peroxide, Ascorbic Acid, MTT reagent (3-(5, 5-dimethylthiazol- 2-yl)-2, 5-diphenyltetrazolium bromide), Dimethyl Sulfoxide (DMSO), Acridine Orange and Ethidium Bromide (Ao/EtBr), Phosphate Buffer Saline (PBS), Rhodamine 123, Propidium Iodide (PI), Mono Dansyl Cadaverine (MDC) and other chemicals and solvents were obtained from Sigma Aldrich (Bangalore, India) and Himedia Ltd (Mumbai, India) with highest purity and used without further purification.

### 3.1Collection of Plant Material

*Tamarindus indica* fruit shells were collected from Koratti village, Tirupattur, Vellore Dt, Tamil Nadu, India, on the basis of cost effectiveness, ease of availability and medicinal property. The collected *Tamarindus indica* shells were rinsed thoroughly first with tap water followed by distilled water to remove all the dust and unwanted visible materials. Then cut into small pieces and dried at room temperature. Then well dried shells are grounded into fine powder for further use.

**3.2Preparation of Plant Extract**

Aqueous extract of *Tamarindus indica* fruit shell was prepared by mixing 10 g fruit shell powder with 100 ml deionized water in the 250 ml Erlenmeyer flask. The mixture was then heated in the hot plate at 60 °C for 20 minutes. The prepared solution was initially filtered through normal filter paper mesh so that the unwanted materials could be filtered out; then the extract was filtered through Whatman filter paper No. 1. The filtered extract was used as the reducing and stabilizing agent in the Nanoparticles synthesis Figure 5.1.

**(a)** **(b)**

**Figure 5.1 (a) *Tamarindus indica* Fruit Shell (b) Aqueous Fruit Shell Extract**

## 5.1 Preliminary Phytochemical Screening

The aqueous fruit shell extract was screened for the presence of alkaloids, saponins, tannins, flavonoids, terpenoids, coumarins, quinones, cardiac glycosides, xanthoproteins, glycosides, steroids, phenols, resins, carboxylic acid group using the standard methods (Harbone (1998); Trease and Evans 1978).

### *5.1.1 Test for Alkaloids*

To identify the alkaloid in the fruit shell extract, the extract was mixed with diluted HCl (1%), warmed and filtered.

#### *5.1.1.1 Mayer's Test:*

Mayer's reagent is containing potassium mercuric iodide. In this test filtrate was mixed with Mayer's reagent. The formation of pale yellow coloured precipitate indicates the presence of alkaloids.

#### *5.1.1.2 Wagner's Test:*

Wagner's reagent contains iodine in potassium iodide. Filtrate was treated with Wagner's reagent and observed for the possible presence of alkaloids by forming brown or reddish precipitate.

### *5.1.2 Test for Saponins (Foam Test)*

The fruit shell extract was mixed with 5.0 ml of distilled water in a test tube and shake vigorously to obtain stable persistent froth. If the froth appeared then it indicates the presence of saponins.

### *5.1.3 Test for Flavonoids*

#### *5.1.3.1 Sodium Hydroxide Test:*

To the fruit shell extract, 2 ml of 2% NaOH was mixed and to develop yellow colour. If the yellow colour becomes colourless after the addition of 2 drops of diluted HCl, it indicates the presence of flavonoids.

#### *5.1.3.2 Shinado's Test:*

To the fruit shell extract, a few pieces of magnesium turnings and few drops of concentrated hydrochloric acid were added and boiled for five minutes. Appearance of pink colour shows the presence of flavonoids.

### *5.1.4 Test for Terpenoids*

To the 5 ml of fruit shell extract, 2.0 ml of chloroform was added. After that 3.0 ml of Conc. $H_2SO_5$ was added. Then the reaction mixture was boiled and cooled. Presence of terpenoids may be confirmed by the formation of blue green or grey colour.

### *5.1.5 Test for Coumarins*

In this test, 2 ml of diluted fruit shell extract was mixed with 2 ml of 10 % NaOH and placed in boiling water bath for few minutes. Appearance of yellow colour indicates the presence of coumarins.

### *5.1.6 Test for Quinones*

In this test, 1 ml of Conc.$H_2SO_5$ was added to the 1 ml of fruit shell extract. The formation of red colour shows the presence of quinones.

### *5.1.7 Test for Tannins*

#### *5.1.7.1 Ferric Chloride Test:*

To the diluted fruit shell extract, a few drops of 0.1 % $FeCl_3$ were added. Appearance of dark green colour indicates the presence of Tannins.

#### *5.1.7.2 Bromine Test:*

In this test, 10 ml of saturated bromine water was added to the 2 ml of diluted fruit shell extract and observe decolouration of bromine water. If decolouration occurs, then it indicates the presence of tannins.

#### *5.1.7.3 Lead Acetate Test:*

About 10 mg of lead acetate was added to the 2 ml of fruit shell extract and shaken well. Formation of white colour precipitate indicates the presence of tannins in the fruit shell extract.

### *5.1.8 Test for Glycosides*

In this test, 2 ml of fruit shell extract was taken and added with 2 ml of glacial acetic acid followed by few drops of $FeCl_3$ and Conc. $H_2SO_5$. Formation of brown ring at the junction of two liquids confirms the presence of glycosides.

### *5.1.9 Test for Xanthoproteins*

To the 2 ml of fruit shell extract, 1 ml of Conc. $H_2SO_5$ was added. A white precipitate will be formed. On boiling the white precipitate it turns to yellow colour. While adding 1 ml of dil. ammonium hydroxide to the solution, yellow colour turns to orange colour and it indicates the presence of xanthoproteins.

### *5.1.10 Test for Steroids*

In this test, 2 ml of fruit shell extract was taken and added to 2 ml of chloroform and Conc. $H_2SO_5$. The formation of red colouration at the lower chloroform layer indicates the presence of steroids.

### *5.1.11 Test for Phenols*

About 2 ml of fruit shell extract was warmed at 55°C and then 2 ml of 0.3% ferric chloride was added. The appearance of green or blue colour confirms the presence of phenols.

### *5.1.12 Test for Resins*

In this test, 2 ml of fruit shell extract was ultra-sonicated for 30 minutes and the formation of turbidity indicates the presence of resins.

#### *5.1.12.1 Molisch's Test*

In this test, 2 ml of fruit shell extract was taken and added 1ml of Molisch's reagent and mixed well. Then few drops of Conc. $H_2SO_5$ was added on the sides of the test tube. Purple ring at the junction of two liquids indicated the presence of carbohydrates.

#### 5.1.12.2 *Fehling's Test:*

To the fruit shell extract, Fehling A and Fehling B reagents were mixed well and boiled. A brick red colour formation in the mixture confirms the presence of carbohydrates.

## 5.2 Green Synthesis of Silver Nanoparticles

10 mM silver nitrate solution was prepared in an Erlenmeyer flask using double distilled water. Then 500 ml of fruit shell extract was added to 100 ml of 10 mM silver nitrate solution and made upto 1000 ml with double distilled water. Then the mixture was stirred for 2 hours at 55 °C by hot plate method with magnetic stirrer.

Reduction of silver ions ($Ag^{+}$) to silver nanoparticles ($Ag^{0}$) was confirmed by the colour change of solution from colourless to brown (Figure 5.2).


**Figure 5.2 Green Synthesis of Silver Nanoparticles using Aqueous Extract of *Tamarindus indica* Fruit Shell**

## 5.3 Characterization of Synthesized Silver Nanoparticles

The reaction mixture was centrifuged for 20 minutes with 5000 rpm and the precipitate was washed with water and centrifuged. Then the pellet was collected and dried in hot air oven with proper temp between 35-50 °C. Dried nanoparticle was collected and used for further characterization and application studies. Nanoparticles are generally characterized by investing their size, shape and surface area. A homogeneity in these properties result in the advancement in applications of Nanoparticles. The characterization of Silver Nanoparticle is done by using various instrumental techniques.

### 5.3.1 UV-Visible Spectrophotometer

The reduction of silver ions to silver nanoparticles was characterized using double beam UV-visible spectrophotometer at wavelength range from 300 nm to 700 nm. This analysis was performed in Perkin Elmer Spectrophotometer (Singapore) and the resolution of instrument is 1 nm. The maximum absorption peaks for *Tamarindus indica* fruit shell extracts and green synthesized silver nanoparticles were recorded.

### 5.3.2 Fourier Transform Infrared Spectroscopy (FTIR)

The IR spectrum of *Tamarindus indica* fruit shell powder and green synthesized silver nanoparticles were performed by FTIR (SHIMADZU instrument). The samples were grinded with KBr pellets and scanned in FTIR spectrum in the range of 5000 – 500 $cm^{-1}$.

### 5.3.3 Scanning Electron Microscope (SEM) and Energy Dispersive Analysis X-Ray (EDAX)

Morphological characters of green synthesized Silver Nanoparticles was analysed by SEM (ZEISS). For this electron microscopic study, the sample was made into thin films by placing on a carbon coated copper grids and the images were recorded. In addition, the presence of elemental silver and other elements in the green synthesized Silver Nanoparticles and fruit shell extract were characterized by Energy Dispersive Spectroscopy (EDS) or Energy Dispersive Analysis X-Ray (EDAX).

### 5.3.4 X-Ray Diffraction (XRD)

Crystalline structure of Silver Nanoparticle was analysed by XRD technique (Model: Philips PW 1830). This instrument operated at a voltage of 50 kV with Cu Kα1 radiation. Crystalline peak was recorded at the 2 θ ranges of 10 - 80°. The average crystalline size of green synthesized Silver Nanoparticle was calculated by using Debye-Scherrer's equation

$$D = \frac{0.9\lambda}{\beta \cos\theta}$$

Here,
D = Particle Size,
λ = X-ray Wavelength,
β = Full Width at Half Maximum (FWHM), θ = Diffraction Angle

### 5.3.5 Transmission Electron Microscope (TEM) and SAED Pattern

The size, shape and dispersal were analyzed using the high-resolution images obtained with transmission electron microscope (TEM) analysis. TEM measurements were measured by TEM-JEOL3010. It is operated at the voltage of 300 kV. The silver nanoparticles were sonicated for 5 min and placed onto copper grid and allowed to dry and images recorded at different magnification power. Selected area diffractogram was used to analyse the crystalline structure of synthesized Silver Nanoparticles.

### 5.3.6 Dynamic Light Scattering (DLS) Analysis

The size distribution intensity of Silver Nanoparticles was measured using the instrument Litesizer™ 500. DLS method gives hydrodynamic diameter values of sample materials. Measurement parameters were as follows: temperature 25 °C, refractive index – 1.3328, viscosity – 0.8878 cp, scattering intensity – 26901 cps and diluent is water. To measure the particle size, a volume of 0.1 ml of the silver nanoparticles solution in 2 ml of deionized water (DI $H_2O$) was placed in a polystyrene cuvette and measured at 25 °C.

## 5.4 Applications of Silver Nanoparticles

### 5.4.1 Antioxidant Activity

Antioxidant activity of synthesized Silver Nanoparticles was carried out by different assays as follows:

a) DPPH Radical Scavenging Assay
b) Hydrogen Peroxide Scavenging Assay
c) Total Antioxidant Capacity Assay

#### 5.4.1.1 DPPH Free Radical Scavenging Assay

The antioxidant activity of green synthesized silver nanoparticles using aqueous fruit shell extract of *Tamarindus indica* was assayed against DPPH free radical by following the method of (Jain and Agrawal, 2008). This assay was performed at different concentration of silver nanoparticles (10 – 50 µg / ml). 10 µl of each concentrations of Silver Nanoparticle sample was taken in different test tubes. 0.659 mM DPPH was dissolved in methanol solution. From this 50 µl was added to all the test tubes and the tubes were incubated at 25 ºC for 20 minutes. The experiment was carried out in triplicates under same condition. After incubation the absorbance of reduced DPPH was recorded at 517 nm using UV-vis spectrophotometer (Shimadzu-1800). Ascorbic acid was used as standard. Same procedure was followed for standard. A test tube containing DPPH solution without sample is considered as control. The percentage of DPPH inhibition was calculated by using the following formula

% Inhibition = [Absorbance of Control – Absorbance of Test Sample / Absorbance of Control] ×100

The 50 % of reduction of free radicals was considered as 50% inhibition

#### 5.4.1.2 Hydrogen Peroxide Scavenging Assay

Hydrogen peroxide scavenging assay was used to determine the free radical scavenging activity. 50 mM of hydrogen peroxide was prepared in 50 mM phosphate buffer (pH 7.5). From this, 0.6 ml was taken in different test tubes and mixed with different concentrations (10 – 50 µg / ml) of synthesized silver nanoparticles using aqueous fruit shell extract of *Tamarindus indica*. Hydrogen peroxide in buffer (without nanoparticles) was maintained as blank and Ascorbic acid was used as standard (Positive Control). Same procedure was followed for standard. All the tubes were incubated at room temperature for 10 min. The absorbance value for determine the percentage of inhibition was measured spectrophotometerically at 230 nm.

ging = [Absorbance of Control – Absorbance of Test Sample / Absorbance of Control] ×100

#### 5.4.1.3 Total Antioxidant Capacity Assay

The total antioxidant capacity of the green synthesized silver nanoparticles using aqueous fruit shell extract of *Tamarindus indica* was assessed spectrophotometrically by the Phospho Molybdenum Method, according to the procedure described by Prieto *et al.*, (1999). Phospho molybdenum reagent was prepared using 0.6 M $H_2SO_5$, 28 mM Sodium phosphate and 5 mM Ammonium molybdate. This assay was performed at different concentration of silver nanoparticles (10 – 50 µg / ml). 10 µl of various concentrations of Silver Nanoparticle sample was taken and mixed with 3 ml of phospho molybdenum reagent. The experiment was carried out in triplicates under same condition. The blank solution contained only 5 ml of reagent solution. A test tube containing phospho molybdenum reagent without sample is considered as blank. Ascorbic acid was used as standard (Positive Control). Same procedure was followed for standard. The mixtures were incubated at 95°C for 150 min. After the mixture had cooled to room temperature, absorbance was measured at 695 nm. The percentage of antioxidant property was calculated by using the following formula

% of Antioxidant Capacity = [(Sample OD – Blank OD) / (Standard OD –

Blank OD)] X 100

### 5.4.2 Catalytic activity of Silver Nanoparticles

#### 5.4.2.1 Dye Degradation - Catalytic Experiments

The catalytic activity of green synthesized Silver Nanoparticle was demonstrated by degrading hazardous dyes such as Safranine O and Methylene blue. In general, 10 mg of each

dye was added to 1 L of distilled water and used as stock solution. After that, 1 mg of green synthesized Silver Nanoparticle was added to 10 ml of each dye solution and mixed ultrasonically for 15 min. Thereafter 3 ml of each mixed solution was used to evaluate the catalytic degradation of dyes. The progress of the reactions was monitored using UV–visible spectrophotometer by measuring absorbance maxima of dyes at different time intervals viz., 30 min, 1 hr, 2 hrs, 8 hrs, 25 hrs and 58 hrs. A control set was maintained without Silver Nanoparticle for each dye and measured for absorbance. The percentage of dye degradation was calculated by the following formula;

Dye degradation percentage (%) = (Initial Absorbance - Final Absorbance)

X 100

Initial Absorbance

### 5.4.3 Antibacterial Activity

Aqueous extract of Tamarind fruit shell mediated synthesized silver nanoparticles was evaluated for its antibacterial property against *Staphylococcus aureus, Bacillus subtilis, Escherichia coli* and *Klebsiella pneumonia* by agar well diffusion assay. Fresh culture (25 hrs) of these above mentioned bacteria are prepared. Antibacterial activity was performed using the media Muller Hinton Agar (MHA). MH agar was freshly prepared and sterilized in autoclave operated at 121°C or 15 lbs for 20 minutes. After sterilization, media was poured into sterile petriplates and allowed to solidify. 100 µL of freshly prepared strain was spread on the plate using L rod. About five wells were made on agar plate using gel puncture with the diameter of 5 mm. Then three different volumes such as 50 µl, 100 µl and 150 µl

(Concentration: 10mg / ml DMSO) of silver nanoparticles were poured into the well separately. DMSO (Dimethyl Sulfoxide) is used as negative control (NC) and commonly available antibiotic gentamycin is used as a positive control (PC). All the plates were incubated at 37 °C for 25 hrs and measure the zone formation around the well.

For the assessment of enhanced antibacterial activity of silver nanoparticles combination with gentamycin was performed by agar well diffusion method. In this method, two wells with 5 mm diameter were made using gel puncture. One well is filled with 5 µL of gentamycin alone and another well is filled with the combination of gentamycin (5 µL) and silver nanoparticles (150 µL). Zone of inhibition around the wells were measured after the incubation. The antibacterial experiment was repeated thrice for concordance.

### 5.4.4 Anticancer Activity

#### 5.4.4.1 Cell culture

The breast cancer cell line (MCF-7) was purchased in NCCS (National Centre for Cell Science), PUNE. These cells were grown in high glucose media DMEM using Fetal Bovine Serum (FBS) (V/V), 100 IU / ml penicillin, 100 mg / ml
streptomycin and 2 mm-glutamine. The cells were grown in 5% $CO_2$ at 37 °C and 95

% humidified atmospheric air.

#### 5.4.4.2 Cell Cytotoxicity (MTT) Assay

The cell cytotoxicity was achieved by the MTT assay (3- (5, 5-dimethylthiazol- 2-yl) - 2, 5-diphenyltetrazolium bromide). The MCF-7 cells are seeded in 96 well plates ($1x10^5$ cells/ well) and allowed to attach overnight. The following morning, old media was aspirated with a new fresh medium which is presented different concentrated silver nanoparticles (0 – 120 µg). The plate system was replaced into an incubator for 25 hrs. After incubation, MTT solution was added to each and every well. The plate was kept under dark condition inside the incubation for 5 hrs. After 5 hrs, the supernatant content was removed and the cells were washed with PBS (200 µl). The purple blue colour formazan was diluted with by adding 100 µl of DMSO. The plate was read at 595 nm in ELISA plate reader. The optical density was used to calculate the percentage of cell cytotoxicity.

## 6. RESULTS AND DISCUSSION

### 6.1 Phytochemical Screening Assay

The phytochemical screening of aqueous extract of fruit shell of *Tamarindus indica* revealed that fruit shell extract have some secondary phyto-compounds such as alkaloids, saponins, flavonoids, carbohydrates, terpenoids, quinones, tannins, glycosides and phenols as shown in Table 6.1. Coumarins, steroids, resins and xanthoproteins were not present in the tamarind fruit shell extract.

A biological activity of plant extract depends on the presence of the secondary metabolites. Bioactivities of the aqueous extract of *Tamarindus indica* fruit shell was based on the presence of some secondary phyto-compounds such as flavonoids, alkaloids, tannins, glycosides and anthroquinones (Watt and Breyer-Brandwijk, 1967; Leven *et al.*, 1979). The natural aromatic phyto-compounds may act as protectors of plant against microbial infection and insects (Marjorie 1999). Anu *et al.*, (2014) reported that the antibacterial efficacy of tamarind pulp is depending on the presence of alkaloids and tannins.

**Table 6.1: Phytochemical Screening of Aqueous Extract of *Tamarindus indica* Fruit Shell**

| Compounds | Test | Result | Present / Absent |
|---|---|---|---|
| Alkaloids | Mayer's Test | Yellow color precipitate | Present |
| | Wagner's Test | Formation of brown precipitate | Present |
| Saponins | Foam Test | formation of froth | Present |
| Flavonoids | Sodium Hydroxide Test | Yellow to colorless | Present |
| | Shinado's Test | Pink color formation | Present |

| | | | |
|---|---|---|---|
| Carbohydrates | Molisch's Test | Purple ring formation | Present |
| | Fehling's Test | Brick red formation | Present |
| Terpenoids | | Blue green color formation | Present |
| Phenols | | Green or blue | Present |
| Quinones | | Red color formation | Present |
| Tannins | Ferric Chloride Test | Dark green appearance | Present |
| | Bromine Test | Decoloration of bromine water | Present |
| | Lead Acetate | White color precipitate | Present |
| Glycosides | | Brown ring | Present |
| Xanthoproteins | Xanthoproteic Test | Orange color | Absent |
| Steroids | Salkowski Test | Red color formed at the lower layer | Absent |
| Yellow color formation | Sodium Hydroxide Test | | Absent |
| Resins | Turbidity Test | Turbid formation | Absent |

## 6.2 GC-MS Analysis

GC-MS method of analysis of phytochemical compound is the most precise methods to identify the presence of secondary metabolites in the extract of plant parts. The plant diversity contains various phytochemicals which is responsible for biological activities that can be considered as valuable therapeutic agents.

The GC-MS analysis has shown the presence of various phytochemical compounds in the aqueous extract of tamarind fruit shell. A total of 26 compounds were identified as shown in Table 6.2.

**Table 6.2: Peak Table of GC-MS Analysis**

| Peak No. | RT | Area (%) | Name of the Compound | Mol. Formula | Mol. Wt | Nature of the compound |
|---|---|---|---|---|---|---|
| 1 | 21.81 | 7.01 | Mome Inositol | $C_7H_{14}O_6$ | 194.00 | Polysaccharide |
| 2 | 21.94 | 4.63 | Mome Inositol | $C_7H_{14}O_6$ | 194.00 | Polysaccharide |
| 3 | 22.02 | 2.66 | Mome Inositol | $C_7H_{14}O_6$ | 194.00 | Polysaccharide |
| 4 | 22.70 | 43.77 | Mome Inositol | $C_7H_{14}O_6$ | 194.00 | Polysaccharide |
| 6 | 22.79 | 10.4 | Mome Inositol | $C_7H_{14}O_6$ | 194.00 | Polysaccharide |
| 6 | 22.87 | 29.00 | Mome Inositol | $C_7H_{14}O_6$ | 194.00 | Polysaccharide |

| | | | | | | |
|---|---|---|---|---|---|---|
| 7 | 23.92 | 0.02 | Acetaldehyde, Ethylhydrazone | $C_4H_{10}N_2$ | 86.14 | Amine compound |
| 8 | 24.62 | 0.09 | 2-Undecanone, 6,10-dimethyl- | $C_{13}H_{26}O$ | 198.34 | Acyclic Hydrocarbon derivative |
| 9 | 26.03 | 0.04 | Pentanoic Acid, Methyl Ester | $C_6H_{12}O_2$ | 116.16 | Aminoacid derivatives |
| 10 | 26.60 | 0.11 | 6-Methylfuro[2,3-C]Pyrid-6-One | $C_8H_7NO_2$ | 133.16 | Pyridine |
| 11 | 26.61 | 0.62 | Hexadecanoic Acid | $C_{16}H_{32}O_2$ | 266.43 | Saturated fatty acid (Palmitate) |
| 12 | 26.86 | 0.03 | 2-Butenoic Acid, 4-Hydroxy-, Methyl Ester | $C_6H_{10}O_3$ | 118.13 | Ester |
| 13 | 28.96 | 0.04 | 2-Hexadecen-1-Ol, 3,7,11,16-Tetramethyl-, [R-[R*,R*-(E)]]- | $C_{20}H_{40}O$ | 296.6 | Acyclic diterpene alcohol (Phytol) |
| 14 | 29.76 | 0.14 | Phenol, 4-Bromo 2-(1,2-Dimethyl-3-Methylenecyclopentyl)-3-Iodo-6-Methyl-, (1R-CIS)- | $C_7H_{13}BrIO$ | 419.96 | Aromatic compound |
| 16 | 34.62 | 0.11 | 2-Methylene-1,6-Pentanediol | $C_6H_{14}O_2$ | 118.17 | Alcoholic compound |
| 16 | 34.86 | 0.42 | 1,2-Benzene dicarboxylic Acid | $C_8H_6O_4$ | 166.13 | Aromatic dicarboxylic acid |

| | | | | | | |
|---|---|---|---|---|---|---|
| 17 | 36.96 | 0.07 | Eicosyl Acetate | $C_{22}H_{44}O_2$ | 340.6 | Ester compound |
| 18 | 37.10 | 0.14 | 4,6,6,6A,10',11'-Hexahydrospiro {6'H-Dibenzo[A,D]Cycloheptene-6',3(3AH)-[4,6,6]Methenocyclopentapyrazole} | $C_{16}H_{12}$ | 192.26 | Hetero cyclic compound |
| 19 | 37.48 | 0.19 | Carbonic acid, bis(2-ethylhexyl) ester | $C_{17}H_{34}O_3$ | 286.4 | Ester compound |
| 20 | 37.76 | 0.02 | 4-(Dimethylamino )Azoestrone 3-Methyl Ether | $C_{21}H_{29}N_3O_2$ | 366.47 | Ether compound |
| 21 | 38.66 | 0.13 | Cyclohexanecarboxylic Acid, 3-(1-Cyano-2-Ethoxy-2-Oxoethylidene) -, Ethyl Ester | $C_{16}H_{26}O_6Si$ | 326.46 | Ester compound |
| 22 | 38.80 | 0.18 | Cyclohexanecarboxylic Acid, 3-(1-Cyano-2-Ethoxy-2-Oxoethylidene) -, Ethyl Ester | $C_{16}H_{26}O_6Si$ | 326.46 | Ester compound |

| | | | | | | |
|---|---|---|---|---|---|---|
| 23 | 38.94 | 0.19 | 2-Propionyl-1-pyrroline | $C_7H_{11}NO$ | 126.17 | Pyrrole and Pyridine derivatives |
| 26 | 39.43 | 0.1 | 3,8,11-Trioxatetracyclo [4.4.1.0(2,4).0(7,9)]undecane, (1.alpha.,2.beta., 4.beta.,6.alpha., 7.beta.,9.beta)- | $C_{16}H_{24}$ | 204.36 | Aliphatic alkanes |

The GC-MS spectrum confirmed the presence of various components with different retention times (Figure 6.1). The mass spectrometer analyzes the compounds eluted at different times to identify the nature and structure of the compounds. The large compound fragments into small compounds giving rise to appearance of peaks at different m/z ratios. These mass spectra are fingerprint of that compound which can be identified from the data library (NIST).

## 6.3 Synthesis of Silver Nanoparticles (SNPs) Using Plants

### 6.3.1Visual Observation

Green synthesized silver nanoparticles using Tamarind fruit shell extract was initially confirmed by visual observation. The silver nanoparticles were formed, when silver nitrate solution was added to fruit shell extract. Initially, the reaction mixture appeared pale yellow in colour and it changed into brown indicates the formation of silver nanoparticles (Figure 6.3). After one hour, the reaction mixture changed into dark brown and finally blackish brown indicating that the reduction of silver ion process was completed. The different colours of silver nanoparticles are related to the excitation effect of surface Plasmon resonance in the reaction mixture. Likewise, prepared nanoparticles
were not aggregate. Several research findings observed that the stability of nanoparticles were extended for more than a week (Sudha *et al.*, 2017; Bindhu and Umadevi, 2013; Chandran *et al.*, 2006).

**(a)** **(b)**

**(c)**

**Figure 6.3: Visual Observation of Tamarind Fruit Shell Extract Mediated Silver Nanoparticles Synthesis (a) Fruit Shell Extract (b) Silver Nitrate Solution (c) Silver Nanoparticles (SNPs)**

## 6.4 Characterization of Synthesized Silver Nanoparticles

### 6.4.1 UV-Visible Absorption Spectrum

The UV-visible absorption spectral study of aqueous extract of Tamarind fruit shell was explored and was depicted in Figure 6.4. The UV-visible spectrum of fruit shell extract was characterized in the range of 260-300 nm in the UV-visible regions. It revealed that a small absorption peak was observed around 280 nm. This region attributed to C=C bond, carbonyl bond and aromatic compounds (Peter Amaladhas *et al.,* 2012; Swarnavalli *et al.,* 2016). These phyto-chemicals plays major role in the reduction of silver ions to SNPs.

UV-visible spectrophotometer is the interesting tool to determine the optical property of silver nanoparticles. The UV-visible spectrum of silver nanoparticles was characterized in the range of 400-640 nm.

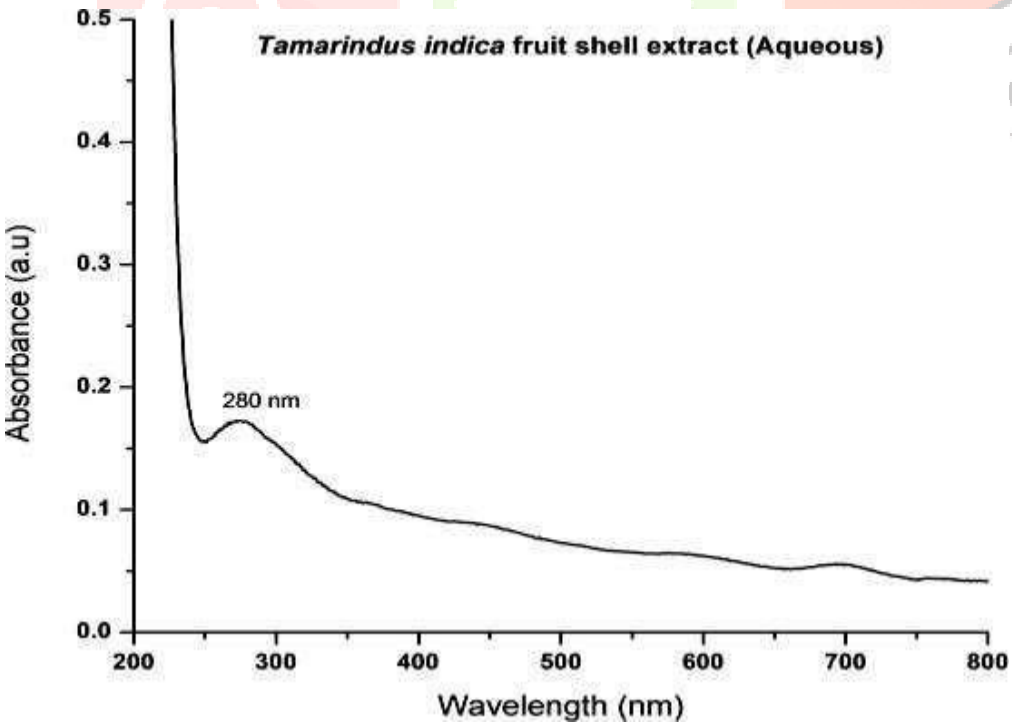


**Figure 6.4: UV-Visible Spectrum of Aqueous Extract of Tamarind Fruit Shell**

UV-visible spectrum illustrates the surface plasmon resonance (SPR) band centered at 460 nm which is characteristics peak for silver nanoparticles (Figure 6.6). It reveals that reduction of silver ions ($Ag^{+}$) to metallic silver nanoparticles.

The SPR band was formed owing to the excitation of free electrons present in the silver nanoparticles while absorbing visible light (Baia *et al.*, 2007). A single peak was observed and that indicates the formation of spherical shape of nanoparticles (He *et al.*, 2002). The broadened peak was displayed and that indicates the poly-dispersed silver nanoparticles (Ashraf *et al.*, 2016) synthesized by using tamarind fruit shells. Similar result was stated on green synthesized silver nanoparticles by Behravan *et al.*, (2019) and Vidhu *et al.*, (2011).

### 5.4.2 FTIR Spectrum

FTIR Spectrum is used to determine the presence of organic molecules on the surface of Nanoparticles. In this present investigation, FTIR measurement was used to identify the phytochemicals present in Tamarind fruit shell extract responsible for reduction of Silver ions to Silver Nanoparticles. FTIR results revealed that similar bands were present in both fruit shell extract and Silver Nanoparticles with slight modifications in wave number (Figure 5.6). Four new peaks were formed and one small peak was disappeared in silver nanoparticles.

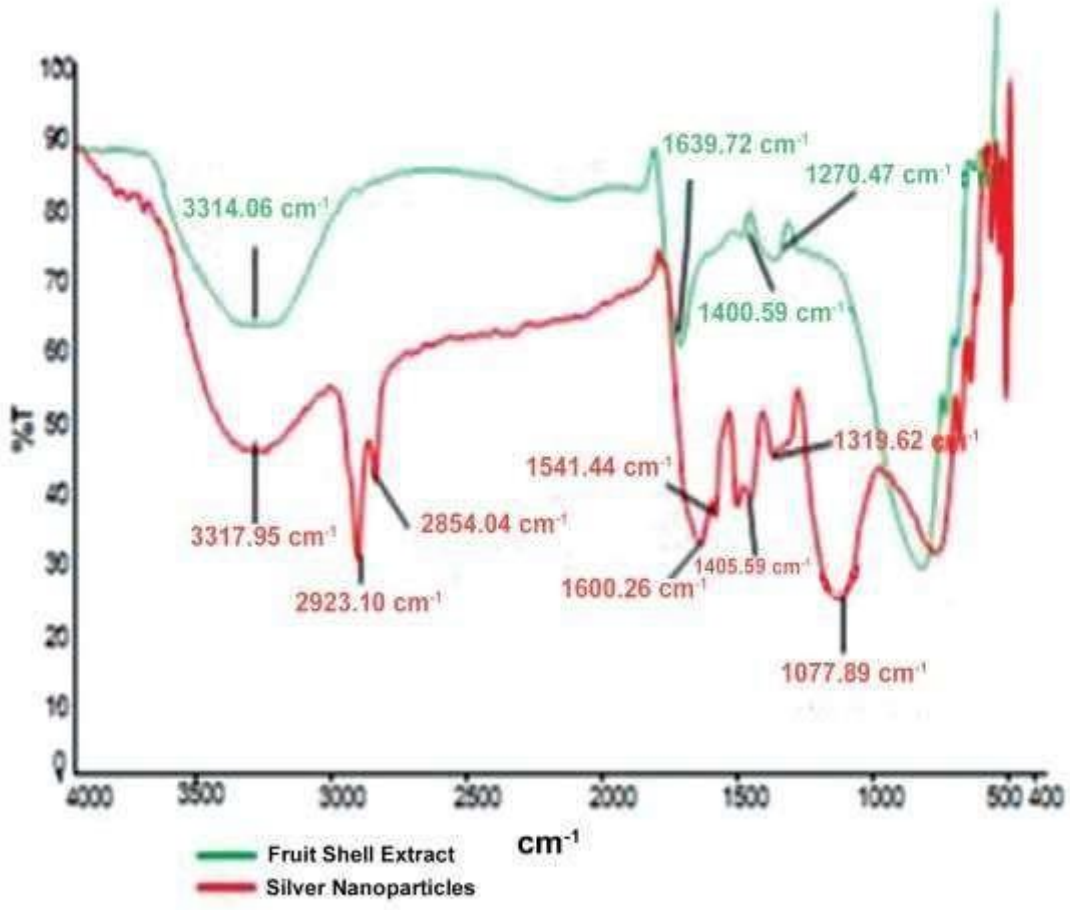


**Figure 5.6: FTIR Spectrum of Tamarind Fruit Shell Extract and Synthesized Silver Nanoparticles**

Fruit shell extract showed a very broad peak at 3314.06 $cm^{-1}$ was changed into 3317.96 $cm^{-1}$ in silver nanoparticles could be assigned to O-H stretching carboxylic acids. Two weak bands are appeared at 2923.10 $cm^{-1}$ and 2864.04 $cm^{-1}$ in silver nanoparticles which corresponds to C–H stretching in alkanes (Table 6.3). A narrow band observed at 1639.72 $cm^{-1}$ assigned to C-C aromatic compounds and N-H primary amines in plant extract (Raghunandan *et al.,* 2010; Stehfest *et al.,* 2006). It was slightly modified into broadened peak at the wave number 1600.26 $cm^{-1}$.

A new peak is formed at the wave number 1641.44 $cm^{-1}$ indicates the presence of N–O asymmetric stretch nitro compounds. The absorption band at 1400 $cm^{-1}$ changed its wave number into 1406.69 $cm^{-1}$ attributed to C–C stretch (in–ring) aromatics. A very weak band was disappeared from plant extract and formed a new peak at 1319.62 $cm^{-1}$ corresponds to C-O stretching alcohols and carboxylic acids (Balashanmugam *et al.,* 2016). Likewise, a new broad band appeared at 1077.89 $cm^{-1}$ related to C–N stretching aliphatic amine group. FTIR result confirmed the presence of carboxyl, alcohol, amine and amide groups in fruit shell extract. These groups may involve in the reduction of Silver ions to Silver Nanoparticles. Only minor changes were seen in between the fruit shell extract and Silver Nanoparticles peak and it suggests that these functional groups play an important role in reducing as well as stabilizing the silver Nanoparticles.

**Table 6.3: Observation Peak Modification of Fruit Shell Extract and Silver Nanoparticles**

| Wave Number ( Fruit Shell Extract ) | Wave Number (Silver Nanoparticles ) | Bond | Molecules | Changes |
|---|---|---|---|---|
| 3314.06 $cm^{-1}$ | 3317.96 $cm^{-1}$ | O-H | Carboxylic Acids | Slight change in wave number |
| | 2923.10 $cm^{-1}$ | C–H stretching | Alkanes | New and weak peak |
| | 2864.04 $cm^{-1}$ | C–H stretching | Alkanes | New and weak peak |
| 1639.72 $cm^{-1}$ | 1600.26 $cm^{-1}$ | C-C & N=H | Aromatic Compounds and Primary Amines | Narrow peak to broad peak and slight changes in wave number |
| | 1641.44 $cm^{-1}$ | N–O asymmetric stretching | Nitro Compounds | New and weak peak |
| 1400.69 $cm^{-1}$ | 1406.69 $cm^{-1}$ | C–C stretching | Aromatics | Slight change in wave number |
| 1270.47 $cm^{-1}$ | - | - | - | Peak disappeared |
| | 1319.62 $cm^{-1}$ | C-O stretching | Alcohols and Carboxylic Acids | Weak peak formed |
| | 1077.89 $cm^{-1}$ | C–N stretching | Aliphatic Amines | New broad peak |

**6.4.3 XRD Spectrum**

Crystalline character and size of green synthesized SNPs was analyzed by X-Ray Diffraction method. XRD spectrum of synthesized SNPs was analyzed with different 2θ ranges from 10° - 80°. XRD pattern shows the peaks at 27.84°, 32.26°, 38.14°, 44.36°,
46.24°, 67.48°, 64.61° and 76.74° which are corresponding to the plane of (210), (113),
(111), (200), (124), (240), (220) and (311) respectively (Figure 6.7). These planes indicate that SNPs are face centered cubic (fcc) crystalline in nature. These observed results are in excellent agreement with the JCPDS File No. 89-3722. Two unassigned peaks were observed at 64.83° and 67.46° due to capping of organic moieties from plant extract on the surface of silver nanoparticles. Similar results were observed on green synthesis of silver nanoparticles by Vanaja and Annadurai (2013) using *Coleus aromaticus* leaf extract and edible mushroom (Daizy, 2009). The average crystalline size of synthesized SNPs was calculated by using Debye - Scherrer's equation

$$D = \frac{0.9\lambda}{\beta \cos\theta}$$

Here,
D = particle size,
λ = X-ray Wavelength,
β = full width at half maximum (FWHM), θ = diffraction angle
The average particle size calculated using diffraction planes are 16 to 60 nm.

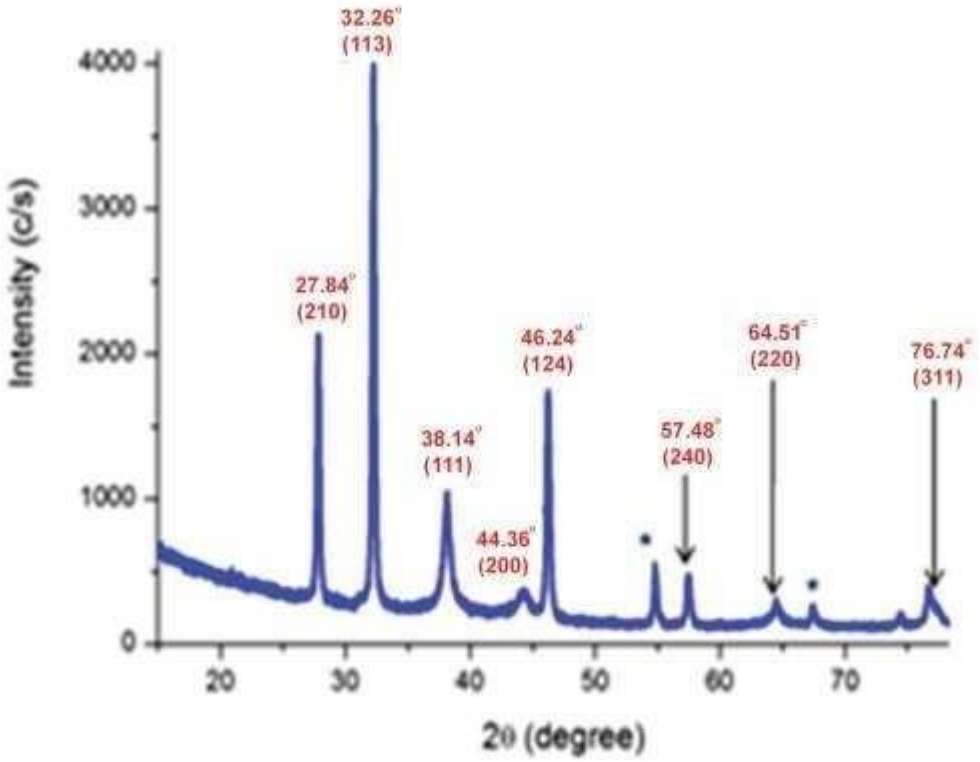


**Figure 5.7: XRD Spectrum of Green Synthesized Silver Nanoparticles**

### 5.4.4 Scanning Electron Microscope (SEM)

Morphological character and size details of the synthesized silver nanoparticles were provided by SEM images. The size of the nanoparticles detected from SEM image range between 20 nm – 52 nm. Similar result was reported by Vanmathi Selvi *et al.*, (2012). This size variation in the nanoparticles is due to the presence of proteins or other molecules from Tamarind fruit shell extract which were bound on the surface of the nanoparticles. And also the result showed that the synthesized silver nanoparticles were of

spherical in shape. Figure 6.8 indicates that the synthesized silver nanoparticles are well separated showing no agglomeration.

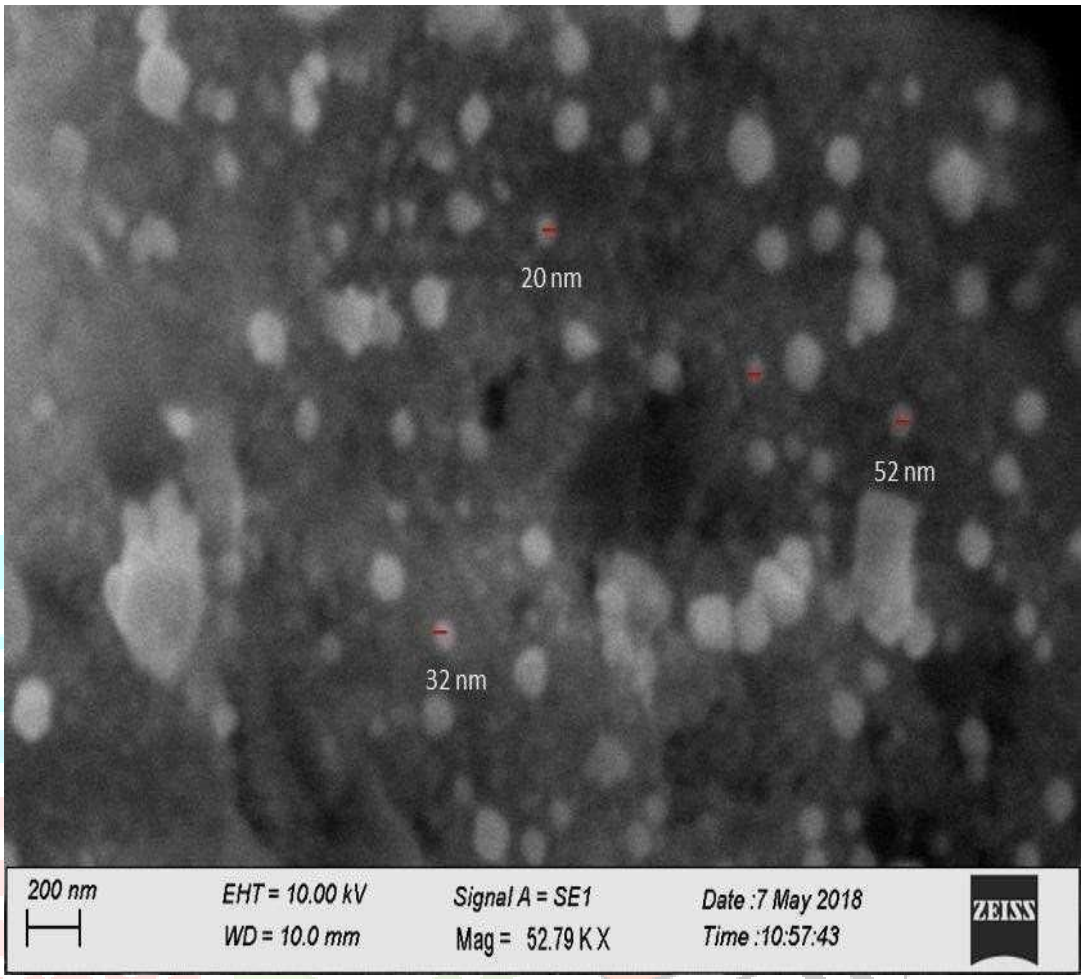


**Figure 6.8: SEM Image of Silver Nanoparticles**

**5.4.5 Energy Dispersive Analysis X-Ray (EDAX)**

Energy Dispersive X-ray Spectrum revealed the composition present in the fruit shell extracts and Silver Nanoparticles. Figure 6.9 shows various elemental composition of fruit shell extract and it includes Ca, K, Na, U and O at various binding energy. These elements were present with biomolecules and responsible for capping on Nanoparticles.

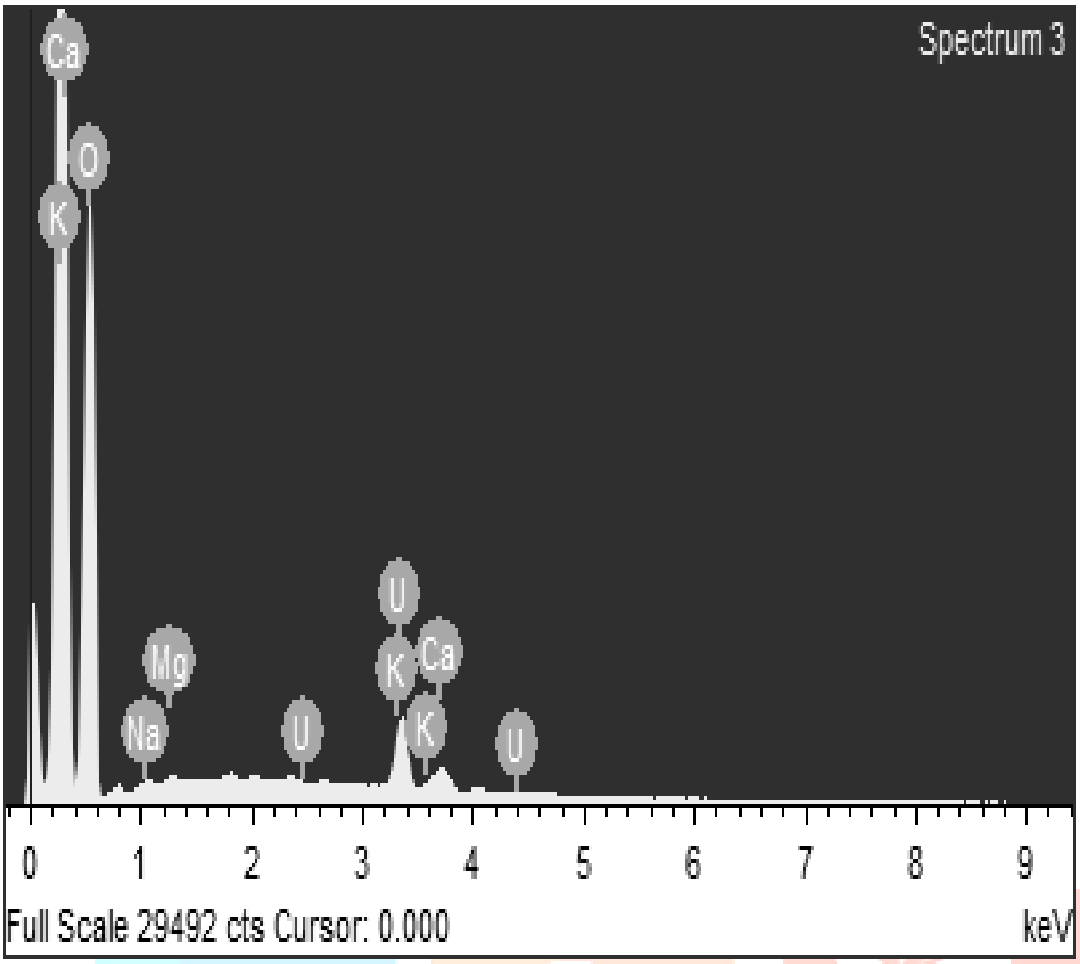


**Figure 6.9: EDAX Spectrum of Tamarind Fruit Shell Extract**

Figure 6.10 represents EDAX of silver nanoparticles and it shows a strong signal peak at 3 keV which is typically for elemental silver. This peak was formed due to the effect of surface plasmon resonance of green synthesized Nanoparticles (Magudapatty et al. 2001). It confirmed the formation of silver Nanoparticles using fruit shell extract.

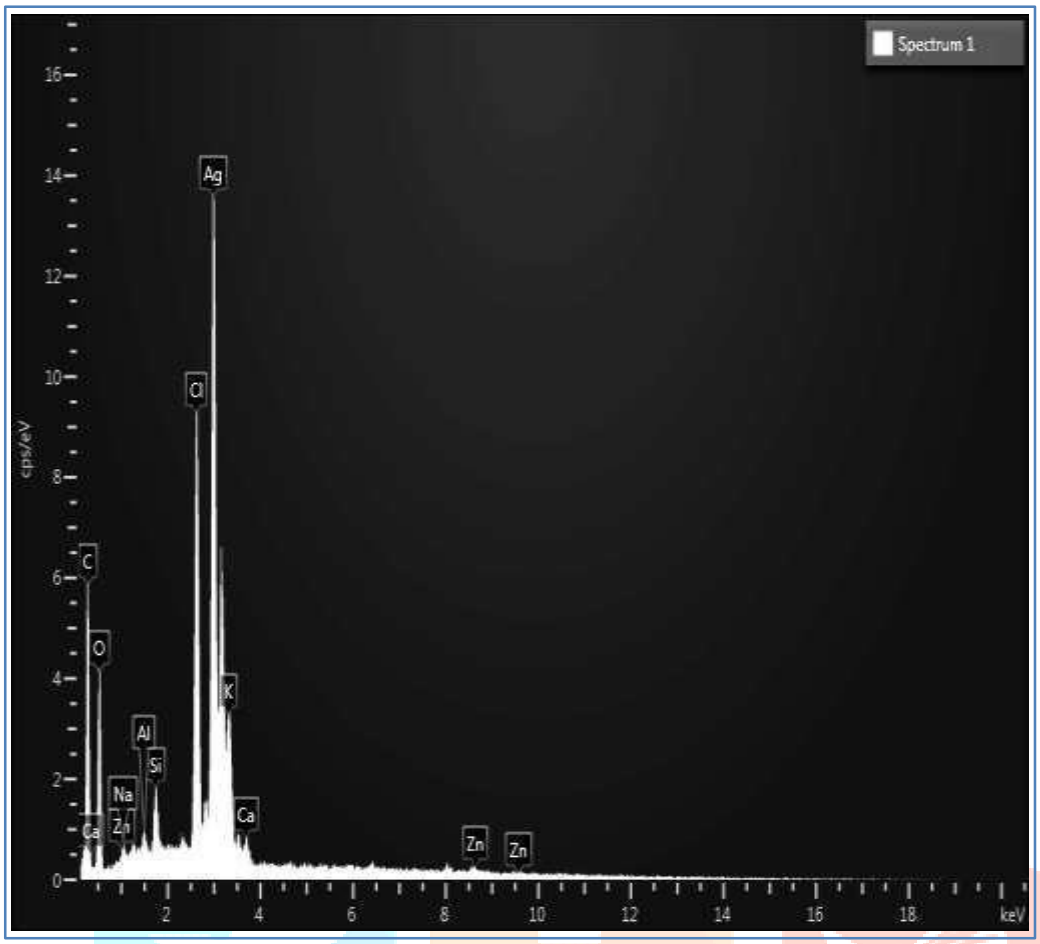


**Figure 6.10: EDAX Spectrum of Silver Nanoparticles**

Other minor peaks such as C, O, Ca, Na, Zn, K and Cl were observed at various absorption energy levels (Table 6.4). These may occur from fruit shell extract due to the presence of moieties of phytochemicals constituents. These components involved in the stabilizing and capping action on the surface of Nanoparticles. Similar results were reported on green synthesis of silver Nanoparticles by Shaik *et al.,* (2018), Anandalakshmi *et al.,* (2016) and Vijayakumar *et al.,* (2013).

**Table 6.4: Composition of (a) Tamarind Fruit Shell Extract and (b) Silver Nanoparticles**

**(a)Tamarind Fruit Shell Extract**

| Element | Line type | Weight % | Atomic % |
|---|---|---|---|
| Na | K series | 3.86 | 5.24 |
| Mg | K series | 3.04 | 3.90 |
| Si | K series | 1.24 | 1.38 |
| P | K series | 1.88 | 1.89 |
| S | K series | 1.70 | 1.66 |
| Cl | K series | 1.93 | 1.70 |
| K | K series | 28.07 | 22.41 |
| Ca | K series | 13.47 | 1.049 |
| Rh | L series | 0.90 | 0.27 |
| U | M series | 19.02 | 2.49 |
| O | | 24.89 | 48.37 |
| **Totals** | | **100** | |

**(b) Silver Nanoparticles**

| Element | Line type | Weight % | Atomic % |
|---|---|---|---|
| C | K series | 28.43 | 53.19 |
| O | K series | 22.24 | 31.24 |
| Na | K series | 0.4 | 0.39 |
| Al | K series | 0.34 | 0.29 |
| Si | K series | 0.92 | 0.73 |
| Cl | K series | 7.44 | 4.72 |
| K | K series | 2 | 1.15 |
| Ca | K series | 0.69 | 0.39 |
| Zn | K series | 0.67 | 0.23 |
| **Ag** | **L series** | **36.87** | **7.68** |
| **Totals** | | **100** | **100** |

**5.4.6 TEM and SAED pattern**

TEM technique was used to determine the size, size distribution and morphological characters of nanoparticles. TEM provide high spatial resolution images.TEM result shows that the synthesized nanoparticles are in nanoscale range and possess uniformity. Also, it shows the size of synthesized nanoparticles, which range between of 20-30 nm and the shape was mostly spherical forms (Figure 6.11).

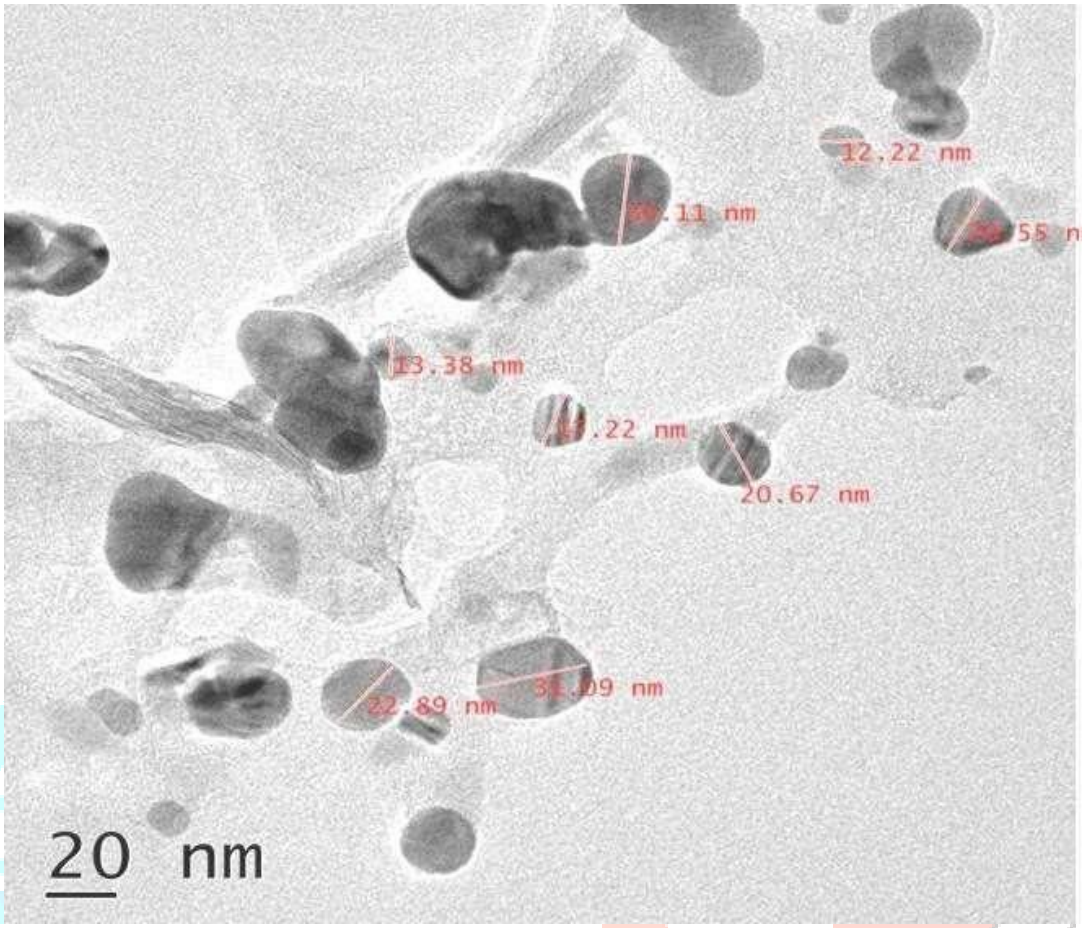


**Figure 6.11: TEM Picture of Synthesized Silver Nanoparticles**

Similar results were reported by other researchers Mittal and Chisti (2013), Singh *et al.*, (2016) and Behravan *et al.*, (2019). Nanoparticles were well dispersed and encapsulated by the fruit shell extract. It was clearly observed from the image. Figure 6.12 depicts the TEM image of biosynthesized silver nanoparticles and showed the well resolved interference fringe patterns separated by 0.17 nm.

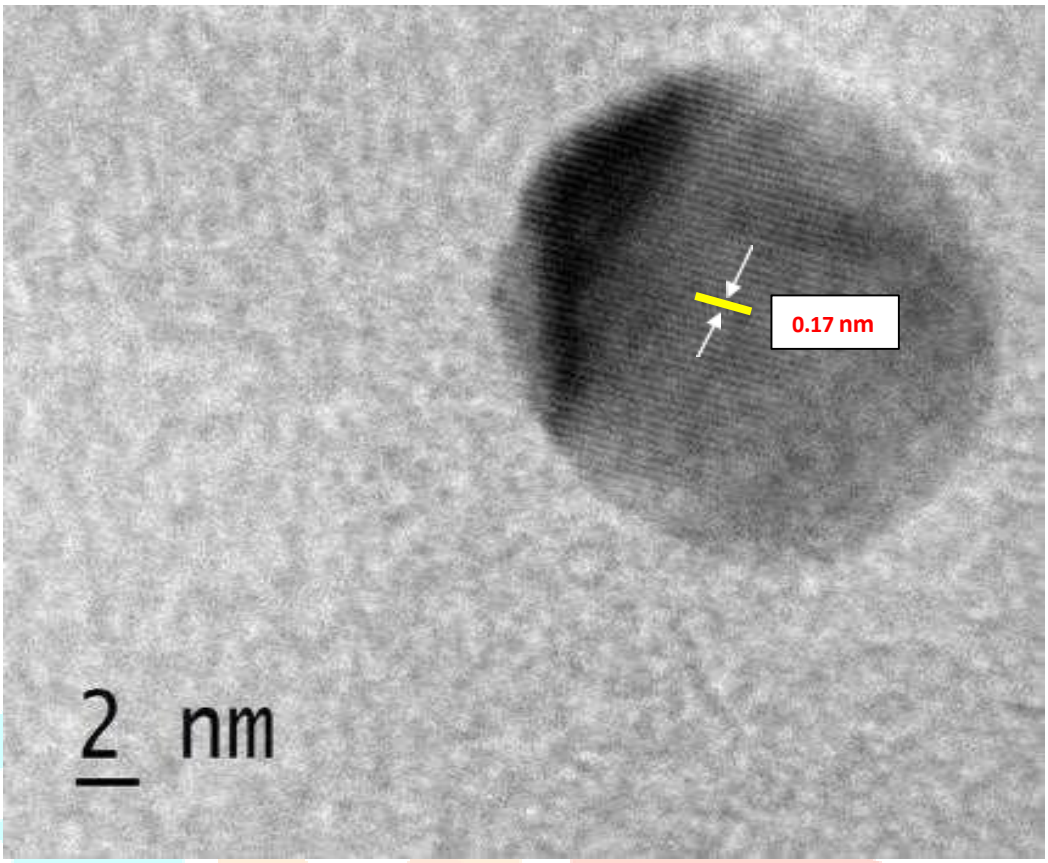


**Figure 6.12: TEM Image of the Single Nanocrystal Entity with Lattice Fringe**

In addition, SAED pattern used to determine the crystalline structure of nanoparticles. This image revealed the ring patterns appeared with the light spots on the dark field. It reflects the crystalline structure of the nanoparticles of silver (Figure 6.13).

**Figure 6.13: SAED Pattern of Synthesized Silver Nanoparticle**

***Table 6.6: Antioxidant Activity of Silver Nanoparticle Determined by DPPH Assay***

| S.No | ncentration ( µg/ml) | Percentage Inhibition (%) | | |
|---|---|---|---|---|
| | | SNP | Ascorbic Acid (Standard) | Fruit Shell Extract |
| 1 | 10 | 61.06 ± 0.26 | 28.67 ± 0.31 | 9.34 ± 0.42 |
| 2 | 20 | 67.80 ± 0.31 | 48.08 ± 0.46 | 11.42 ± 0.23 |
| 3 | 30 | 63.36 ± 0.12 | 66.26 ± 0.61 | 14.16 ± 0.61 |
| 4 | 40 | 66.01 ± 0.22 | 82.86 ± 0.26 | 19.01 ± 0.32 |
| 6 | 60 | 72.41 ± 0. 43 | 92.74 ± 0.34 | 22.23 ± 0.46 |

**Mean ± SD**

**Table 6.6: Antioxidant Activity of SNP Determined by $H_2O_2$ Assay**

| S.No | ncentration ( µg/ml) | Percentage Inhibition (%) | | |
|---|---|---|---|---|
| | | SNP | Ascorbic Acid (Standard) | Fruit Shell Extract |
| 1 | 10 | 47.33 ± 0.24 | 44.66 ± 0.37 | 10.34 ± 0.12 |
| 2 | 20 | 60.00 ± 0.17 | 63.08 ± 0.26 | 17.42 ± 0.23 |
| 3 | 30 | 63.73 ± 0.41 | 66.12 ± 0.31 | 19.16 ± 0.61 |
| 4 | 40 | 77.20 ± 0.37 | 82.23 ± 0.21 | 23.01 ± 0.26 |
| 6 | 60 | 87.86 ± 0.43 | 91.14 ± 0.14 | 27.23 ± 0.46 |

**Mean ± SD**

### *5.5.2 Antibacterial Activity of Silver Nanoparticles*

#### *5.5.2.1 Antibacterial Activity of SNP against Pathogenic Bacteria*

Agar well diffusion method was adopted to investigate the antibacterial activity of tamarind fruit shell extract mediated silver nanoparticles synthesis. The activity was calculated by formation of zone around the well and expressed in millimeter (mm) in diameter. Triplicate experiment was performed to find out the statistical error. The zone of inhibition was measured against *Staphylococcus aureus, Bacillus subtilis, Escherichia coli* and *Klebsiella pneumoniae* shown in Figure 6.22.

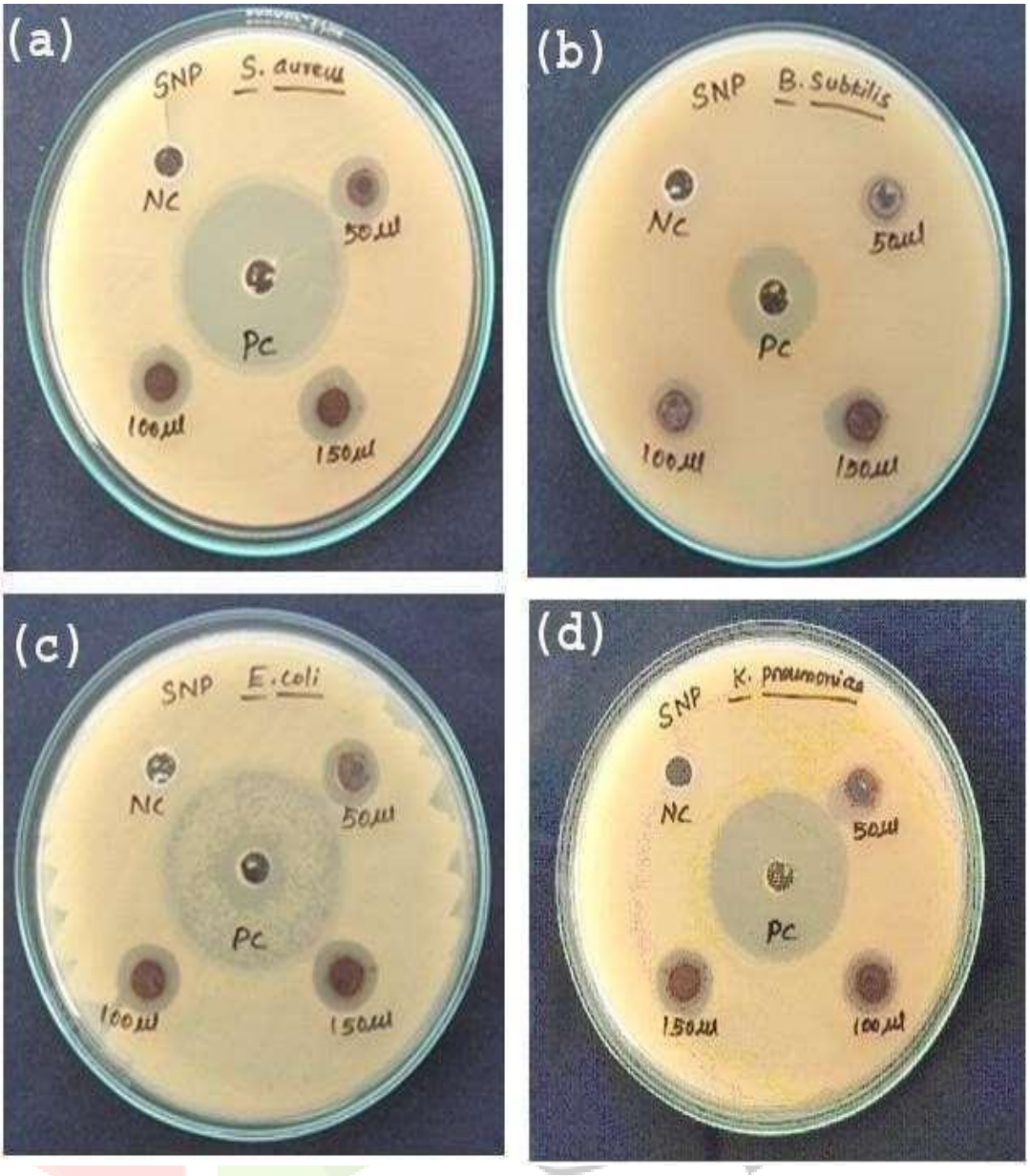


**Figure 6.22: Antibacterial Activity of Silver Nanoparticles Synthesized using Tamarind Fruit Shell Extract against Four Pathogenic Bacteria's (a) *Staphylococcus aureus*, (b) *Bacillus subtilis, (c) Escherichia coli* and (d) *Klebsiella pneumoniae***

*5.5.2.2 Comparison of Green Synthesized Silver Nanoparticles with Positive (Gentamycin) and Negative (DMSO) Control*

Three different concentrations (60 µl, 100 µl and 160 µl) of silver nanoparticles were loaded. The negative control (without nanoparticles) and positive control (Gentamycin) were used for the comparison study of antibacterial activity. Figure 6.23 and Table 6.9 confirms that zone formation against pathogenic bacteria was increased at increasing the concentration of silver nanoparticles. The bioactivity is performed based on the concentration dependent manner.

**Table 6.9: Zone of Inhibition Produced by Green Synthesized Silver Nanoparticles (SNPs) against Test Organisms as Compared with Positive and Negative Control**

| **Concentration** | **Zone of Inhibition of Green Synthesized Silver Nanoparticles (mm in diameter)** | | | |
|---|---|---|---|---|
| | ***S.aureus*** | ***B.subtilis*** | ***E.coli*** | ***K.pneumoniae*** |
| Negative Control (DMSO) | 0 | 0 | 0 | 0 |
| Positive Control (Gentamycin) | 17 ± 2.60 | 10 ± 2.60 | 18 ± 2.60 | 16 ± 2.10 |
| 60 µl SNPs | 07 ± 1.70 | 06 ± 1.70 | 06 ± 1.20 | 06 ± 1.70 |
| 100 µl SNPs | 07 ± 1.00 | 06 ± 0.60 | 07 ± 1.00 | 06 ± 0.69 |
| 160 µl SNPs | 08 ± 0.60 | 07 ± 1.00 | 08 ± 1.70 | 07 ± 1.00 |

**Mean ± SD**

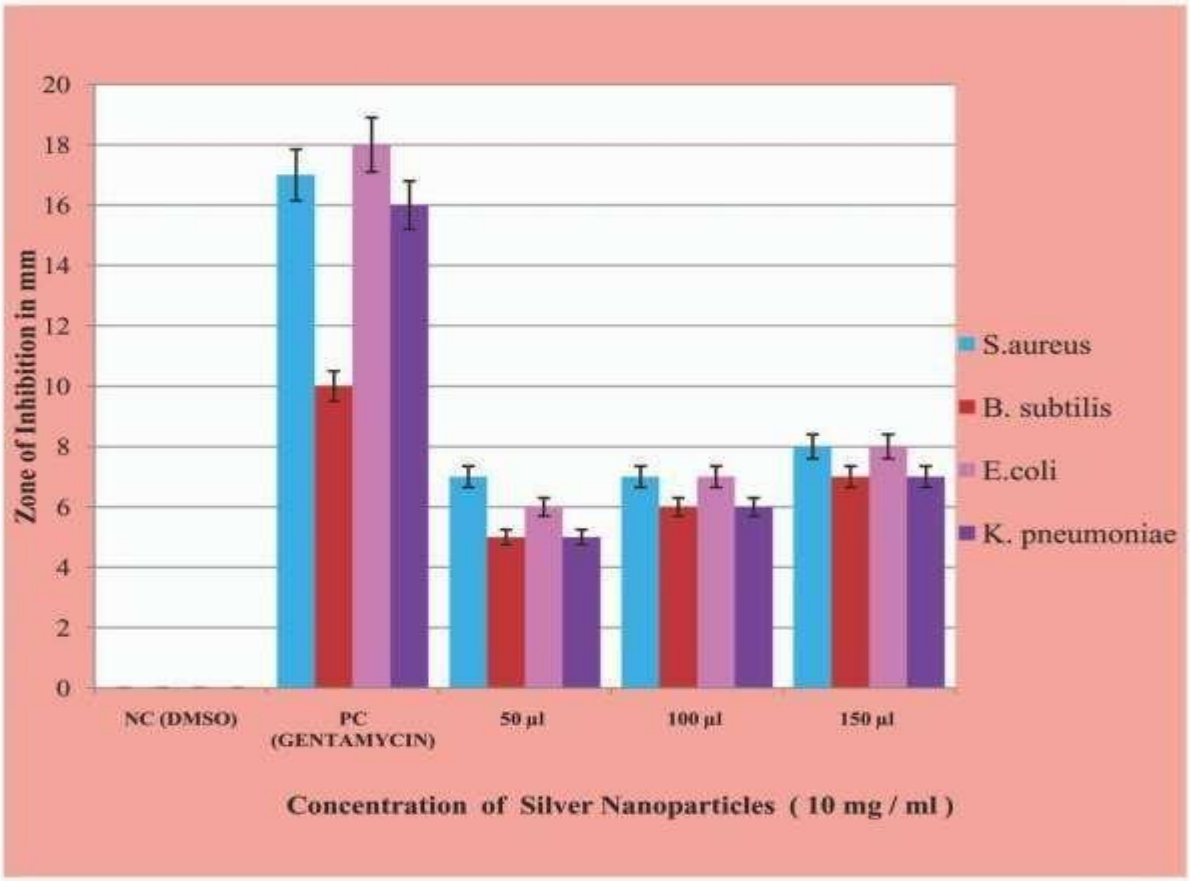


**Figure 5.23: Antibacterial Activity of Silver Nanoparticles Synthesized by Tamarind Fruit Shell Extract against Test Organisms**



Shivajirao Pawar College o Highest zone of inhibition was observed at 160 µl concentration of SNP and the zone of inhibition is found to be 08 ± 0.60, 07 ± 1.00, 08 ± 1.70, and 07 ± 1.00 mm in diameter against *S.aureus*, *B.subtilis*, *E.coli* and *K.pneumoniae* respectively. The negative control (DMSO) did not form any zone of inhibition. Highest zone of inhibition was noted against *S.aureus* and *E.coli* and they are highly sensitive to silver nanoparticles. Lowest inhibition was noted against *B.subtilis* and *K.pneumoni* f Pharmacy, Pachegaon 56

## 9. References


1. Iravani S. Green synthesis of metal nanoparticles using plants. Green Chem. 2011;13(10):2638–2650.
2. Li X, Xu H, Chen ZS, Chen G. Biosynthesis of nanoparticles by microorganisms and their applications. J Nanomater. 2011;2011:1–16.
3. Parashar V, Parashar R, Sharma B, Pandey AC. Parthenium leaf extract mediated synthesis of silver nanoparticles. Dig J Nanomater Biostruct. 2009;4(1):45–50.
4. Husen A, Siddiqi KS. Plants and microbes assisted selenium nanoparticles: characterization and application. J Nanobiotechnol. 2014;12:28.
5. Behravan M, Panahi AH, Naghizadeh A, et al. Facile green synthesis of silver nanoparticles using Berberis vulgaris. Artif Cells Nanomed Biotechnol. 2019;47(1):113–120.
6. Jemilugba OT, Sakho EH, Parani S, Mavumengwana V. Green synthesis of silver nanoparticles using Combretum erythrophyllum leaf extract. Colloids Surf B Biointerfaces. 2019;178:465–473.
7. Mitiku AA, Yilma B. Green synthesis of silver nanoparticles using Moringa stenopetala leaf extract. J Nanotechnol. 2017;2017:1–8.
8. Al-Sheddi ES, Farshori NN, Al-Oqail MM, et al. Anticancer potential of green synthesized silver nanoparticles using Nepeta deflersiana. Bioinorg Chem Appl. 2018;2018:1–12.
9. Roy K, Sarkar CK, Ghosh CK. Green synthesis of silver nanoparticles using Azadirachta indica. Appl Nanosci. 2017;7(1):95–104.
10. Logaranjan K, Raiza AJ, Gopinath SCB, Chen Y. Shape-controlled synthesis of silver nanoparticles using Aloe vera extract. Mater Lett. 2016;180:1–4.
11. Tippayawat P, Phromviyo N, Boueroy P, Chompoosor A. Green synthesis of silver nanoparticles using Aloe vera. Green Process Synth. 2016;5(2):173–180.
12. Rastogi L, Arunachalam J. Sunlight based synthesis of silver nanoparticles using garlic extract. Mater Chem Phys. 2011;129:558–563.
13. Moodley JS, Krishna SBN, Pillay K. Green synthesis of silver nanoparticles from Moringa oleifera. J Photochem Photobiol B. 2018;188:126–133.
14. Giron-Vazquez NG, et al. Green synthesis of silver nanoparticles using Persea americana seed extract. Nanomaterials. 2019;9:1–14
15. Oves M, Aslam M, Rauf MA, et al. Antimicrobial and anticancer activities of silver nanoparticles synthesized using Phoenix dactylifera. Saudi J Biol Sci. 2018;25(2):226–234.
16. Keshari AK, Srivastava R, Singh P, et al. Green synthesis of silver nanoparticles using Cestrum nocturnum. J Clust Sci. 2018;29:1–8.
17. Ahn EY, Jin H, Park Y. Antioxidant and cytotoxic properties of plant mediated silver nanoparticles. Mater Sci Eng C. 2019;101:204–216.
18. Mahendran D, Ranjithakumari B. Green synthesis of silver nanoparticles using Nothapodytes nimmoniana fruit. J Nanostruct Chem. 2016;6:1–8.
19. Jain S, Mehata MS. Medicinal plant mediated synthesis of nanoparticles. Sci Rep. 2017;7:15867.
20. Sudha A, Jeyakanthan J, Srinivasan P. Synthesis of silver nanoparticles using Lippia nodiflora. Spectrochim Acta A. 2017;173:151–157.
21. Luna-Sanchez RM, et al. Jalapeno chili mediated synthesis of silver nanoparticles. J Nanomater. 2019;2019:1–10.
22. Pirtarighat S, Ghannadnia M, Baghshahi S. Green synthesis of silver nanoparticles using Salvia spinosa. Appl Nanosci. 2019;9:1–10.
23. Ashraf A, Zafar S, Zahid K, et al. Synthesis and characterization of silver nanoparticles using Coriandrum sativum. Appl Nanosci. 2019;9:1839–1849.
24. Logeswari P, Silambarasan S, Abraham J. Green synthesis of silver nanoparticles using medicinal plants. Spectrochim Acta A. 2015;141:86–93.
25. Moldovan B, David L, Achim M, et al. Green synthesis of silver nanoparticles using Sambucus nigra. J Mol Liq. 2016;221:271–278.
26. Hazarika SN, Das P, Bharali P. Green synthesis of silver nanoparticles using Thalictrum foliolosum. Mater Lett. 2016;178:151–154.
27. Reddy NJ, Vali DN, Rani M, Rani SS. Evaluation of antioxidant and antibacterial activity of silver nanoparticles using Piper longum. J Nanostruct Chem. 2014;4:1–8.
28. Gurunathan S, Kalishwaralal K, Vaidyanathan R, et al. Biosynthesis of silver nanoparticles using E. coli. Colloids Surf B Biointerfaces. 2009;74:328–335.
29. Mukherjee P, Ahmad A, Mandal D, et al. Fungus-mediated synthesis of silver nanoparticles. Nano Lett. 2002;2(5):515–519.
30. Sastry M, Ahmad A, Khan MI, Kumar R. Biosynthesis of metal nanoparticles using fungi and actinomycetes. Curr Sci. 2005;85:162–17